JAERI - M
87-061

INITIAL RESULTS OF LOWER HYBRID CURRENT DRIVE EXPERIMENT ON JT-60

May 1987

Keishi SAKAMOTO, Tsuyoshi IMAI, Yoshitaka IKEDA, Kazuya UEHARA
Tsuneyuki FUJII, Mikio SAIGUSA, Masao HONDA, Norio SUZUKI
Kenji YOKOKURA, Masami SEKI, Masaki TSUNEOKA, Masayuki SAWAHATA
Kazuaki SUGANUMA, Sunao MAEBARA, Kimihiro KIYONO, Haruyuki KIMURA
Katsuto ANNO, Masayuki TERAKADO, Takashi NAGASHIMA
Hirohumi SHIRAKATA, Masato AKIBA, Takeshi FUKUDA, Yuzuru NEYATANI
Takeo NISHITANI, Kenkichi USHIGUSA, Ryuji YOSHINO and JT-60 team

日 本 原 子 力 研 究 所
Japan Atomic Energy Research Institute

JAERI-Mレポートは，日本原子力研究所が不定期に公刊している研究報告書です。
入手の問合わせは，日本原子力研究所技術情報部情報資料課（〒319-11茨城県那珂郡東海村）あて，お申しこしください。なお，このほかに財団法人原子力弘済会資料センター（〒319-11茨城県那珂郡東海村日本原子力研究所内）で複写による実費頒布をおこなっております。

JAERI-M reports are issued irregularly.
Inquiries about availability of the reports should be addressed to Information Division, Department of Technical Information, Japan Atomic Energy Research Institute, Tokai-mura, Naka-gun, Ibaraki-ken 319-11, Japan.

編集兼発行　日本原子力研究所
印　　刷　㈱原子力資料サービス

JAERI-M 87-061

Initial Results of Lower Hybrid Current Drive Experiment on JT-60

Keishi SAKAMOTO, Tsuyoshi IMAI, Yoshitaka IKEDA, Kazuya UEHARA
Tsuneyuki FUJII, Mikio SAIGUSA, Masao HONDA, Norio SUZUKI
Kenji YOKOKURA, Masami SEKI, Masaki TSUNEOKA, Masayuki SAWAHATA
Kazuaki SUGANUMA, Sunao MAEBARA, Kimihiro KIYONO, Haruyuki KIMURA
Katsuto ANNO, Masayuki TERAKADO, Takashi NAGASHIMA
Hirohumi SHIRAKATA, Masato AKIBA, Takeshi FUKUDA, Yuzuru NEYATANI
Takeo NISHITANI, Kenkichi USHIGUSA, Ryuji YOSHINO and JT-60 team

Department of large Tokamak Research
Naka Fusion Research Establishment
Japan Atomic Energy Research Institute
Naka-machi, Naka-gun, Ibaraki-ken

(Received March 19, 1987)

The initial results of current drive experiment by lower hybrid range of frequencies (LHRF) on JT-60 are reported. This experiment is a first trial of RF current drive on a reactor grade tokamak. As the result, the current of 1.7MA is driven by LHRF with the power of 1.2MW (2.0GHz) at the density $\bar{n}_e = 0.3 \times 10^{19}$ m^{-3}. The efficiency of current drive $\eta_{CD}(\equiv \bar{n}_e(10^{19}\ m^{-3})\ I_{RF}(MA)R(m)/P_{RF}(MW))$ is $0.7 \sim 1.7$. When neutral beams are combined with LHRF, η_{CD} increased to $2.0 \sim 2.8$. Furthermore, current ramp up and recharging were carried out. The efficiencies of current ramp up and recharging are approximately 0.2 for both. Also, the suppression of soft X-ray sawtooth signals is recognized, as obserbed on middle sized tokamak.

Keywords: JT-60, Lower Hybrid Current Drive, Neutral Beams.

JT-60 Team

M. YOSHIKAWA, T. ABE, H. AKAOKA, H. AIKAWA, H. AKASAKA, M. AKIBA
N. AKINO, T. AKIYAMA, T. ANDO, K. ANNOH, N. AOYAGI, K. ARAKAWA
M. ARAKI, K. ARIMOTO, M. AZUMI, S. CHIBA, M. DAIRAKU, N. EBISWA
T. FUJII, T. FUKUDA, H. FURUKAWA, K. HAMAMATSU, K. HAYASHI, M. HARA
K. HARAGUCHI, H. HIRATSUKA, T. HIRAYAMA, S. HIROKI, K. HIRUTA, M. HONDA
H. HORIIKE, R. HOSODA, N. HOSOGANE, Y. IIDA, T. IIJIMA, K. IKEDA
Y. IKEDA, T. IMAI, T. INOUE, N. ISAJI, M. ISAKA, S. ISHIDA, N. ITIGE
T. ITO, Y. ITO, A. KAMINAGA, M. KAWAI, Y. KAWAMATA, K. KAWASAKI
K. KIKUCHI, M. KIKUCHI, H. KIMURA, T. KIMURA, H. KISHIMOTO, K. KITAHARA
S. KITAMURA, A. KITSUNEZAKI, K. KIYONO, N. KOBAYASHI, K. KODAMA
Y. KOIDE, T. KOIKE, M. KOMATA, I. KONDO, S. KONOSHIMA, H. KUBO
S. KUNIEDA, S. KURAKATA, K. KURIHARA, M. KURIYAMA, T. KURODA, M. KUSAKA
Y. KUSAMA, S. MAEHARA, K. MAENO, S. MATSUDA, S. MASE, M. MATSUKAWA
T. MATSUKAWA, M. MATSUOKA, N. MIYA, K. MIYATI, Y. MIYO, K. MIZUHASHI
M. MIZUNO, R. MURAI, Y. MURAKAMI, M. MUTO, M. NAGAMI, A. NAGASHIMA
K. NAGASHIMA, T. NAGASHIMA, S. NAGAYA, H. NAKAMURA, Y. NAKAMURA
M. NEMOTO, Y. NEYATANI, S. NIIKURA, H. NINOMIYA, T. NISHITANI
H. NOMATA, K. OBARA, N. OGIWARA, T. OHGA, Y. OHARA, K. OHASA
H. OHHARA, T. OHSHIMA, M. OHKUBO, K. OHTA, M. OHTA, M. OHTAKA
Y. OHUCHI, A. OIKAWA, H. OKUMURA, Y. OKUMURA, K. OMORI, S. OMORI
Y. OMORI, T. OZEKI, A. SAKASAI, S. SAKATA, M. SATOU, M. SAIGUSA
K. SAKAMOTO, M. SAWAHATA, M. SEIMIYA, M. SEKI, S. SEKI, K. SHIBANUMA
R. SHIMADA, K. SHIMIZU, M. SHIMIZU, Y. SHIMOMURA, S. SHINOZAKE
H. SHIRAI, H. SHIRAKATA, M. SHITOMI, K. SUGANUMA, T. SUGIE, T. SUGIYAMA
H. SUNAOSHI, K. SUZUKI, M. SUZUKI, M. SUZUKI, N. SUZUKI, S. SUZUKI
Y. SUZUKI, M. TAKAHASHI, S. TAKAHASHI, T. TAKAHASHI, H. TAKAHASHI*
M. TAKASAKI, M. TAKATSU, H. TAKEUCHI, A. TAKESHITA, S. TAMURA
S. TANAKA, K. TANI, M. TERAKADO, T. TERAKADO, K. TOBITA, T. TOKUTAKE
T. TOTSUKA, N. TOYOSHIMA, H. TSUDA, T. TSUGITA, S. TSUJI, Y. TSUKAHARA
M. TSUNEOKA, K. UEHARA, M. UMEHARA, Y. URAMOTO, H. USAMI, K. USHIGUSA
K. USUI, J. YAGYU, K. YAMADA, M. YAMAMOTO, O. YAMASHITA, Y. YAMASHITA
K. YANO, T. YASUKAWA, K. YOKOKURA, H. YOKOMIZO, H. YOSHIDA
Y. YOSHINARI, R. YOSHINO, I. YONEKAWA and K. WATANABE

* Plasma Physics Laboratory, Princeton University, USA

JAERI-M 87-061

ＪＴ－60における低域混成波電流駆動実験の初期結果

日本原子力研究所那珂研究所臨界プラズマ研究部
坂本　慶司・今井　　剛・池田　佳隆・上原　和也・藤井　常幸
三枝　幹雄・本田　正男・鈴木　紀男・横倉　賢治・関　　正美
恒岡まさき・沢畠　正之・菅沼　和明・前原　　直・清野　公広
木村　晴行・安納　勝人・寺門　正之・永島　　孝・白形　弘文
秋場　真人・福田　武司・閨谷　　譲・西谷　健夫・牛草　健吉
芳野　隆治・ＪＴ－60チーム

（1987年3月19日受理）

ＪＴ－60における低域混成波（ＬＨＲＦ）による電流駆動実験の初期結果の報告である。この実験は，核融合炉クラスのトカマクにおけるＲＦ電流駆動の初の試みであるが，その結果，電子密度 $\bar{n}_e = 0.3 \times 10^{19}\,m^{-3}$ のプラズマにおいて入射電力1.2MWのＬＨＲＦ（周波数2GHz）によりプラズマ電流 $I_{RF} = 1.7$ MAの駆動に成功した。これは現在までの非誘導型電流駆動実験で得られたものとしては世界最高の値である。なお，電流駆動効率 η_{CD}（$\equiv n_e(10^{19}m^{-3}) \times I_{RF}$（MA）・R（m）／$P_{RF}$（MW）は1.0～1.7であるが，中性粒子入射（ＮＢＩ）と組み合わせた時，η_{CD}は2.0～2.8に上昇した。

さらにＬＨＲＦによるプラズマ電流立ち上げ実験及びＯＨコイル電流の再充電実験を行い，効率としてそれぞれ $\eta_{ramp} = 0.2$，$\eta_{recharge} = 0.2$ を得た。

また，中型装置において観測されたＬＨＲＦによる軟Ｘ線上の鋸歯状振動の抑制も確認された。

那珂研究所：〒311－02　茨城県那珂郡那珂町大字向山801－1

JT－60 チーム

相川　裕史，青柳　哲雄，赤岡　伸雄，赤坂　博美，秋野　昇，秋場　真人，秋山　隆，
安積　正史，阿部　哲也，新井　貴，荒川喜代次，荒木　政則，有本　公子，安東　俊郎，
安納　勝人，飯島　勉，飯田　幸生，池田　幸治，池田　佳隆，井坂　正義，伊佐治信明，
石田　真一，市毛　尚志，伊藤　孝雄，伊藤　康浩，井上多加志，今井　剛，上原　和也，
宇佐美広次，牛草　健吉，薄井　勝富，梅原　昌敏，浦本　保幸，海老沢　昇，及川　晃，
大麻　和美，大内　豊，大賀　徳道，大久保　実，大島　貴幸，太田　和也，太田　充，
大高　光夫，大原比呂志，大森憲一郎，大森　俊造，大森　栄和，荻原　徳男，奥村　裕司，
奥村　義和，小関　隆久，小原建治郎，小原　祥裕，神永　敦嗣，河合視己人，川崎　幸三，
川俣　陽一，菊池　勝美，菊池　満，岸本　浩，北原　勝美，北村　繁，狐崎　晶雄，
木村　豊秋，木村　晴行，清野　公廣，日下　誠，草間　義紀，国枝　俊介，久保　博孝，
倉形　悟，栗原　研一，栗山　正明，黒田　猛，小池　常之，小出　芳彦，児玉　幸三，
木島　滋，小林　則幸，小又　将夫，近藤　育朗，三枝　幹雄，逆井　章，坂田　信也，
坂本　慶司，佐藤　正泰，沢畠　正之，蔀　守正，篠崎　信一，柴沼　清，嶋田　隆一，
清水　勝宏，清水　正亜，下村　安夫，白井　浩，白形　弘文，菅沼　和明，杉江　達夫，
杉山　隆，鈴木　貞明，鈴木　国弘，鈴木　紀男，鈴木　正信，鈴木　道雄，鈴木　康夫，
砂押　秀則，清宮　宗孝，関　省吾，関　正美，高崎　学，高津　英幸，高橋　春次，
高橋虎之助，高橋　弘法*，高橋　実，竹内　浩，竹下　明，田中　茂，田中竹次郎，
谷　啓二，田村　早苗，大楽　正幸，千葉　真一，塚原　美光，次田　友宜，辻　俊二，
津田　文男，恒岡まさき，寺門　恒久，寺門　正之，徳竹　利国，戸塚　俊之，飛田　健次，
豊島　昇，中村　博雄，中村　幸治，長島　章，永島　圭介，永島　孝，永谷　進，
永見　正幸，新倉　節夫，西谷　健夫，二宮　博正，根本　正博，閨谷　譲，野亦　英幸，
濱松　清隆，林　和夫，原　誠，原口　和三，平塚　一，平山　俊雄，蛭田　和治，
広木　成治，福田　武司，藤井　常幸，古川　弘，細金　延幸，細田隆一郎，堀池　寛，
本田　正男，前野　勝樹，前原　直，間瀬　修次，松岡　守，松川　達哉，松川　誠，
松田慎三郎，水野　誠，水橋　清，宮　直之，宮地　謙吾，三代　康彦，武藤　貢，
村井　隆一，村上　義夫，柳生　純一，安川　亨，矢野　勝久，山下　修，山下　幸彦，
山田喜美雄，山本　正弘，横倉　賢治，横溝　英明，吉川　和伸，吉川　允二，吉田　英俊，
吉成　洋治，芳野　隆治，米川　出，渡辺　和弘，

＊プリンストン大学プラズマ物理研究所，米国

Contents

1. Introduction 1
2. RF Heating System of JT-60 1
3. Current Drive at the MA Level and Recharging/Current Ramp up 2
4. Improvement of Current Drive Efficiency by NBI 4
5. Current Profile during LHCD and Suppression of MHD Mode 5
6. Summary 7
Acknoledgement 7
References 8

目　　次

1. 序 1
2. ＪＴ－60におけるＲＦ加熱装置 1
3. ＭＡレベル電流駆動及び再充電／電流立ち上げ実験 2
4. ＮＢＩによる電流駆動効率の改善 4
5. ＬＨＣＤ中の電流分布及びＭＨＤモードの抑制 5
6. 要　約 7
謝　辞 7
参考文献 8

1. Introduction

A large number of current drive or current start up and ramp up experiments by LHRF have been successfully performed on the small or middle sized tokamaks which have opened a new way for CW operation of the tokamak[1-11]. Further intersting results, i.e. the current profile during LHCD is formed independently with the T_e profile[12], and the sawtooth of soft X-ray can be suppressed by LHCD via fattening of the current profile, are reported[13-15]. These results have to be tested on a reactor sized tokamak and the potential of LHCD has to be demonstrated in order to give guidance for the design of a fusion reactor. Also, the combination of LHCD and other additional heating on large tokamaks is an important theme. In view of these needs, the LHCD experiment on JT-60, which is a large tokamak with a poloidal divertor having a major radius of 3.1m and minor radius of 0.9m, is carried out as the first application of current drive to a reactor sized tokamak.

In this paper, the results of the first phase experiment of LHCD on JT-60 are presented. The experiment was carried out stressing the following points;

(1) demonstration of MA class current drive,
(2) estimation of current drive efficiency,
(3) current drive in conbination with NBI.

In section 2, the RF heating system is described in brief. Next, the experimental results of current drive, recharging and current ramp up are given in section 3. The reuslt of current drive in the combination with NBI is presented in section 4, and the current profile during current drive and MHD mode suppression are discussed in section 5. The summary is presented in section 6.

2. RF Heating System of JT-60

The RF heating system has three units for LHRF heating and current drive and one unit of ICRF heating. One launcher of the LHRF units is designed for current drive(LHCD). Each unit of LHRF is composed of a RF generating system, high power RF amplifier system having eight 1MW klystrons, RF transmission system of 32 waveguides, coupling system, differential pumping system for the coupling system, cooling system,

1. Introduction

A large number of current drive or current start up and ramp up experiments by LHRF have been successfully performed on the small or middle sized tokamaks which have opened a new way for CW operation of the tokamak[1-11]. Further intersting results, i.e. the current profile during LHCD is formed independently with the T_e profile[12], and the sawtooth of soft X-ray can be suppressed by LHCD via fattening of the current profile, are reported[13-15]. These results have to be tested on a reactor sized tokamak and the potential of LHCD has to be demonstrated in order to give guidance for the design of a fusion reactor. Also, the combination of LHCD and other additional heating on large tokamaks is an important theme. In view of these needs, the LHCD experiment on JT-60, which is a large tokamak with a poloidal divertor having a major radius of 3.1m and minor radius of 0.9m, is carried out as the first application of current drive to a reactor sized tokamak.

In this paper, the results of the first phase experiment of LHCD on JT-60 are presented. The experiment was carried out stressing the following points;

(1) demonstration of MA class current drive,
(2) estimation of current drive efficiency,
(3) current drive in conbination with NBI.

In section 2, the RF heating system is described in brief. Next, the experimental results of current drive, recharging and current ramp up are given in section 3. The reuslt of current drive in the combination with NBI is presented in section 4, and the current profile during current drive and MHD mode suppression are discussed in section 5. The summary is presented in section 6.

2. RF Heating System of JT-60

The RF heating system has three units for LHRF heating and current drive and one unit of ICRF heating. One launcher of the LHRF units is designed for current drive(LHCD). Each unit of LHRF is composed of a RF generating system, high power RF amplifier system having eight 1MW klystrons, RF transmission system of 32 waveguides, coupling system, differential pumping system for the coupling system, cooling system,

power supply system and control/diagnostics system. The layout of the RF heating system is illustrated in Fig. 1 and one LHRF unit is shown schematically in Fig. 2. The maximum generator power of one unit is 8MW and more than 5MW is expected as injection power into the tokamak. The frequency of RF can be choosed every 500msec among five values, 1.74, 1.83, 2.0, 2.17, 2.23GHz, by selecting the frequency of the RF generator and shifting the tunner of the 1MW klystrons. Also, the RF power and phase difference between adjacent waveguides can be changed with the time step of 10msec by controlling the RF generating system. The control signals are sent every 10msec from the RF computer or JT-60 computer called ZENKEI via a CAMAC system. The launcher is a Grill type having the 4×8 waveguides as shown in Fig. 3(a). The inner sizes of the waveguides of LHCD launcher is 16mm×115mm. The power spectrum of the waves injected from the LHCD launcher is shown in Fig. 3(b). The peak of the wavenumber spectrum along the magnetic field is $N_{//} = 1.7$ with the width $\Delta N_{//} \sim 1$ at $\Delta\phi = 90°$.

3. Current Drive at the MA Level and Recharging/Current Ramp up

Experiments were performed in both hydrogen and helium plasmas in the parameter range $\bar{n}_e = 0.2 - 4.0 \times 10^{19}$ m^{-3}, $I_p = 0.5 - 2.0$MA, $B_T = 4$T, $q_{eff} = 3.7 - 11$. In the helium discharges the hydrogen was always employed as the prefilling gas so that the helium plasmas contain a hydrogen minority. A torus input power of LHRF up to 1.4MW was injected at a frequency of 2GHz. The hydrogen NB, having the port through power up to 20MW with the beam energy of 40 - 70keV, was injected almost perpendicular to the LHCD plasma. The RF parameters are as follows; frequency f = 2.0GHz, phase difference $\Delta\phi = 60° \sim 120°$ (mainly 90°), distance between plasma center and top of the launcher R = 945 ~ 950mm. (The fixed limiter is placed at R = 940mm.)

Fig. 4 shows the typical data of current drive experiment under I_p constant control at $P_{LH} = 1$MW, $B_T = 4$T with hydrogen plasma. Fig. 4(a) ~ (e) are time dependences of plasma current I_p, one turn voltage V_1, density $\bar{n}_e$, Shafranov lambda Λ and current of the OH primary coil I_F. LHRF is injected with two pulses, first from t = 3.0 ~ 3.5sec and second from t = 4.0 ~ 8.0sec as shown in (a). The one turn voltage drops from 1.0V to 0V or slightly negative level during LHRF injection. The

power supply system and control/diagnostics system. The layout of the RF heating system is illustrated in Fig. 1 and one LHRF unit is shown schematically in Fig. 2. The maximum generator power of one unit is 8MW and more than 5MW is expected as injection power into the tokamak. The frequency of RF can be choosed every 500msec among five values, 1.74, 1.83, 2.0, 2.17, 2.23GHz, by selecting the frequency of the RF generator and shifting the tunner of the 1MW klystrons. Also, the RF power and phase difference between adjacent waveguides can be changed with the time step of 10msec by controlling the RF generating system. The control signals are sent every 10msec from the RF computer or JT-60 computer called ZENKEI via a CAMAC system. The launcher is a Grill type having the 4×8 waveguides as shown in Fig. 3(a). The inner sizes of the waveguides of LHCD launcher is 16mm×115mm. The power spectrum of the waves injected from the LHCD launcher is shown in Fig. 3(b). The peak of the wavenumber spectrum along the magnetic field is $N_{//} = 1.7$ with the width $\Delta N_{//} \sim 1$ at $\Delta\phi = 90°$.

3. Current Drive at the MA Level and Recharging/Current Ramp up

Experiments were performed in both hydrogen and helium plasmas in the parameter range $\bar{n}_e = 0.2 - 4.0 \times 10^{19}$ m^{-3}, $I_p = 0.5 - 2.0$MA, $B_T = 4$T, $q_{eff} = 3.7 - 11$. In the helium discharges the hydrogen was always employed as the prefilling gas so that the helium plasmas contain a hydrogen minority. A torus input power of LHRF up to 1.4MW was injected at a frequency of 2GHz. The hydrogen NB, having the port through power up to 20MW with the beam energy of 40 - 70keV, was injected almost perpendicular to the LHCD plasma. The RF parameters are as follows; frequency f = 2.0GHz, phase difference $\Delta\phi = 60° \sim 120°$ (mainly 90°), distance between plasma center and top of the launcher R = 945 ~ 950mm. (The fixed limiter is placed at R = 940mm.)

Fig. 4 shows the typical data of current drive experiment under I_p constant control at $P_{LH} = 1$MW, $B_T = 4$T with hydrogen plasma. Fig. 4(a) ~ (e) are time dependences of plasma current I_p, one turn voltage V_l, density $\bar{n}_e$, Shafranov lambda Λ and current of the OH primary coil I_F. LHRF is injected with two pulses, first from t = 3.0 ~ 3.5sec and second from t = 4.0 ~ 8.0sec as shown in (a). The one turn voltage drops from 1.0V to 0V or slightly negative level during LHRF injection. The

plasma current is maintained at the 1MW level even after LHRF injection due to the I_p = constant feedback control; however, the ohmic current is replaced by the RF current I_{RF}. The level of I_{RF} is evaluated as $I_{RF} = |\Delta V_1/V_1| I_p$, so $I_{RF} = I_p = 1$MA as $|\Delta V_1/V_1| \sim 1$. In fact, $dI_F/dt = 0$ during RF injection, which means I_p is maintained by RF power only. The value of $\bar{n}_e$ is kept nearly constant level during RF injection. The transition of Λ will be discussed later. When $\bar{n}_e$ is low, V_1 stays negative, and recharging of the OH coil current occurs($dI_F/dt > 0$). This result is shown in Fig. 5(a) - (d). In this shot, LHRF power of $P_{LH} = 0.57$MW was injected to the plasma of $\bar{n}_e \sim 0.2 \times 10^{13}$ m^{-3}, $I_p = 0.7$MA and the recharging efficiency can be estimated. The rising time of OH coil current I_F is 1.3kA/sec, therefore, the recharging efficiency defined as $\eta_{recharge} = I_p \dot{I}_f M/P_{RF} = 0.2$. Here, the mutual inductance between plasma and OH coil of JT-60 is $M = 140\mu$H. In the estimation of recharging efficiency, the effect of changing l_i is not taken into account. Therefore, a longer RF pulse duration will be needed to obtain a more accurate measurement of recharging efficiency. Fig. 6(a), (b) shows the results of current sustainment and current ramp up by LHCD under the condition where I_p is not constant. Fig. 6(a) shows that $dI_F/dt = 0$ at $t \geq 3.4$sec, which indicates $\bar{n}_e$ and I_p are maintained by LHRF only. Fig. 6(b) is a case that LHRF is injected into a plasma whose I_p is decreasing. This figure clearly shows I_p increase again simultaneously with LHRF injection. These results are very important as a demonstration of the current sustain and ramp up by LHCD only in a reactor-grade tokamak. In Fig. 7, the ramp up efficiency η_{ramp} is shown. η_{ramp} is defined by the relation of $dW_{PF}/dt - P_{ext} = \eta_{ramp} P_{LH} - D$. Here, dW_{RF}/dt ($=d/dt(1/2 L_p I_p^2)$) is the increase rate of stored energy of poloidal magnetic field, P_{ext} is energy of poloidal field except from RF power and D is power loss of RF via plasma. The ordinate and abscissa are $dW_{PF}/dt - P_{ext}$ and P_{LH}, respectively, and the gradient of the solid line in the figure indicates the ramp up efficency. Though a precise estimate is difficult because of the limited amount of valid data in our experiment, we obtain the value of $\eta_{ramp} = 0.2$, which is reasonable comparing the value $\eta_{ramp} = 0.1 \sim 0.2$ in PLT.

Fig. 8 shows the result of 1.7MA of driven current with LHRF power injection of 1.2MW into a plasma of $\bar{n}_e = 0.3 \times 10^{19}$ m^{-3} and $I_p = 2$MA. The value of V_1 drops from 1.1V to 0.15V, therefore, $\Delta V_1 = 0.95$V, which

corresponds to $I_{RF} = 1.7$MA. This is the largest noninductive current obtained to date on any tokamak, including current drive by NBI.

The efficiency of current drive η_{CD} is defined usually as

$$\eta_{CD} = \bar{n}_e(10^{19}\ m^{-3})R(m)I(MA)/P_{LH}(MW)\ [17].$$

Up to now, the values of $\eta_{CD} = 0.7 \sim 1.5$ are obtained in LHCD experiments on the small or middle sized tokamaks.

Figs. 9(a), (b) show the dependences of $I_p\Delta V_1/V_1/P_{LH}(\sim I_{RF}/P_{LH})$ on $\bar{n}_e$ carried out in LHCD experiment with the filling gases of H and He, respectively. The closed and open symbols in the figures mean the cases of $|\Delta V_1/V_1| < 1$ and $|\Delta V_1/V_1| > 1$, respectively. $|\Delta V_1/V_1| < 1$ indicates the existence of some OH electric field contributing to the current drive. Both figures show the I_{RF}/P_{LH} are in inverse proportion to $\bar{n}_e$. The current drive efficiency at $|\Delta V_1/V_1| > 1$ is lower than the case of $|\Delta V_1/V_1| < 1$, especially in He discharge. This may depend on the decrease of resistivity of the plasma due to accelerated electrons produced by LHRF. In fact, the theory predicts that enhancement of conductivity including the effect of fast electrons in He plasma is about 1.5 times higher than H discharge, which show the agreement with the experimental results [16,17,18].

4. Improvement of Current Drive Efficiency by NBI

Now, let us consider the reason why η_{CD} of JT-60 is high compared with the other machines. The Fisch's theory predicts the difference of η_{CD} among the machine is little if the parameters are optimized. Therefore, the present theory cannot explain the result obtained in JT-60 and we have to explore another reason. One possible idea is the effect of electron temperature, which does not include explicitly in the theory. Generally, there are gaps between phase velocity of LHRF v_{ph} and electron thermal velocity v_{th} (spectrum gap), therefore, the electrons have to be accelerated up to v_{ph}. So, it can be predicted if the spectrum gap is large, η_{CD} becomes low, and if that is small, η_{CD} becomes high.

According to this expedition, LHCD experiment was tried with combination of electron heating by NBI. Fig. 10 is a typical data of time dependencies of plasma parameters in OH+LHCD+NBI shots. LHRF is injected into the plasma of $I_p = 1$MA from t=4.0sec with the power of

corresponds to $I_{RF} = 1.7$MA. This is the largest noninductive current obtained to date on any tokamak, including current drive by NBI.

The efficiency of current drive η_{CD} is defined usually as

$$\eta_{CD} = \bar{n}_e(10^{19}\ m^{-3})R(m)I(MA)/P_{LH}(MW)\ [17].$$

Up to now, the values of $\eta_{CD} = 0.7 \sim 1.5$ are obtained in LHCD experiments on the small or middle sized tokamaks.

Figs. 9(a), (b) show the dependences of $I_p\Delta V_1/V_1/P_{LH}(\sim I_{RF}/P_{LH})$ on $\bar{n}_e$ carried out in LHCD experiment with the filling gases of H and He, respectively. The closed and open symbols in the figures mean the cases of $|\Delta V_1/V_1| < 1$ and $|\Delta V_1/V_1| > 1$, respectively. $|\Delta V_1/V_1| < 1$ indicates the existence of some OH electric field contributing to the current drive. Both figures show the I_{RF}/P_{LH} are in inverse proportion to $\bar{n}_e$. The current drive efficiency at $|\Delta V_1/V_1| > 1$ is lower than the case of $|\Delta V_1/V_1| < 1$, especially in He discharge. This may depend on the decrease of resistivity of the plasma due to accelerated electrons produced by LHRF. In fact, the theory predicts that enhancement of conductivity including the effect of fast electrons in He plasma is about 1.5 times higher than H discharge, which show the agreement with the experimental results [16,17,18].

4. Improvement of Current Drive Efficiency by NBI

Now, let us consider the reason why η_{CD} of JT-60 is high compared with the other machines. The Fisch's theory predicts the difference of η_{CD} among the machine is little if the parameters are optimized. Therefore, the present theory cannot explain the result obtained in JT-60 and we have to explore another reason. One possible idea is the effect of electron temperature, which does not include explicitly in the theory. Generally, there are gaps between phase velocity of LHRF v_{ph} and electron thermal velocity v_{th} (spectrum gap), therefore, the electrons have to be accelerated up to v_{ph}. So, it can be predicted if the spectrum gap is large, η_{CD} becomes low, and if that is small, η_{CD} becomes high.

According to this expedition, LHCD experiment was tried with combination of electron heating by NBI. Fig. 10 is a typical data of time dependencies of plasma parameters in OH+LHCD+NBI shots. LHRF is injected into the plasma of $I_p = 1$MA from t=4.0sec with the power of

P_{LH} = 0.88MW, and successively NB of P_{NBI} = 8.8MW is injected from t = 4.8sec as shown in the figure. The drop of V_1 change by NBI, i.e. $|\Delta V_1/V_1|$ = 1.25 before NBI and $|\Delta_1/V_1|$ = 0.75 during NBI. These values correspond to I_{RF} of 1.25MA, 0.75MA, respectively. On the other hand, $\bar{n}_e$ increase from 0.35×10^{19} m^{-3} to 0.9×10^{19} m^{-3} by NBI. These indicate the change of η_{CD} from 1.5 to 2.4. The current drive efficiency of LHCD only (○) and LHCD + NBI (●) are summarized in $P_{LH}/\bar{n}_e$ dependencies of I_{RF} in Fig. 11. The solid lines in the figure mean the current drive efficiencies of η_{CD} = 1.0,2.0,3.0. In the case of LHCD only, η_{CD} lies from 1.0 to 1.7, however, as clearly shown in the figure, η_{CD} is improved to 2.0 ~ 2.8 when NBI heating is combined.

In Fig. 12, the temperature dependences of current drive efficiencies with the data of other machines are shown [19]. The range of electron temperature $\bar{T}_e$ during LHCD on JT-60 is $\bar{T}_e$=1.05~2.5keV for OH+LHCD and $\bar{T}_e$ = 1.45 ~ 3.1keV for OH + LHCD + NBI. The dashed lines in the figure mean the value of a characteristic current drive efficiency $\hat{j}/\hat{P}(=\tau/\tau_0 v_{te}/(\omega/k)$, $\tau_0=4\pi\varepsilon_0{}^2 m_e{}^2 v_{te}{}^3/(n_e e^4 \ln\Lambda)$, $\tau=6\pi(2\pi)^{1/2}\varepsilon_0{}^2 m_e{}^{1/2} T_e{}^{3/2}/(n_i Z_i{}^2 e^4 \ln\Lambda)$. These data indicate that the current drive efficiency increases with temperature.

5. Current Profile during LHCD and Suppression of MHD Mode

The current by LHCD is formed by high velocity electrons accerelated by LHRF wave via Landau damping. Therefore, the plasma current profile of LHCD may be largely different from the current profile driven by OH. As the current profile of JT-60 cannot be measured directly, it was deduced by other indirect methods. Among them, the time dependence of Λ sometimes gives us useful information of the change of current profile. In Fig. 13(a), the typical result of time dependences of V_1, Λ is shown. As the magnitude of β_p is small compared with l_i in this density region, we regard that $2d\Lambda/dt \sim dl_i/dt$, which indicates the change of current profile. The values of Λ increases during 200msec after LHRF injection and subsequently decreases gradually. The final value of Λ is lower than initial value of Λ. On the other hand, V_1 starts to decrease after LHRF injection with a time lag of 200msec. From these data, the current profile is estimated using the diffusion equation of poloidal magnetic field [20]. The

P_{LH} = 0.88MW, and successively NB of P_{NBI} = 8.8MW is injected from t = 4.8sec as shown in the figure. The drop of V_1 change by NBI, i.e. $|\Delta V_1/V_1|$ = 1.25 before NBI and $|\Delta_1/V_1|$ = 0.75 during NBI. These values correspond to I_{RF} of 1.25MA, 0.75MA, respectively. On the other hand, $\bar{n}_e$ increase from 0.35×10^{19} m^{-3} to 0.9×10^{19} m^{-3} by NBI. These indicate the change of η_{CD} from 1.5 to 2.4. The current drive efficiency of LHCD only (○) and LHCD + NBI (●) are summarized in $P_{LH}/\bar{n}_e$ dependencies of I_{RF} in Fig. 11. The solid lines in the figure mean the current drive efficiencies of η_{CD} = 1.0,2.0,3.0. In the case of LHCD only, η_{CD} lies from 1.0 to 1.7, however, as clearly shown in the figure, η_{CD} is improved to 2.0 ~ 2.8 when NBI heating is combined.

In Fig. 12, the temperature dependences of current drive efficiencies with the data of other machines are shown [19]. The range of electron temperature $\bar{T}_e$ during LHCD on JT-60 is $\bar{T}_e$=1.05~2.5keV for OH+LHCD and $\bar{T}_e$ = 1.45 ~ 3.1keV for OH + LHCD + NBI. The dashed lines in the figure mean the value of a characteristic current drive efficiency $\hat{j}/\hat{P}(= \tau/\tau_0 v_{te}/(\omega/k)$, $\tau_0 = 4\pi\varepsilon_0^2 m_e^2 v_{te}^3/(n_e e^4 \ln\Lambda)$, $\tau = 6\pi(2\pi)^{1/2}\varepsilon_0^2 m_e^{1/2} T_e^{3/2}/(n_i Z_i^2 e^4 \ln\Lambda)$. These data indicate that the current drive efficiency increases with temperature.

5. Current Profile during LHCD and Suppression of MHD Mode

The current by LHCD is formed by high velocity electrons accerelated by LHRF wave via Landau damping. Therefore, the plasma current profile of LHCD may be largely different from the current profile driven by OH. As the current profile of JT-60 cannot be measured directly, it was deduced by other indirect methods. Among them, the time dependence of Λ sometimes gives us useful information of the change of current profile. In Fig. 13(a), the typical result of time dependences of V_1, Λ is shown. As the magnitude of β_p is small compared with l_i in this density region, we regard that $2d\Lambda/dt \sim dl_i/dt$, which indicates the change of current profile. The values of Λ increases during 200msec after LHRF injection and subsequently decreases gradually. The final value of Λ is lower than initial value of Λ. On the other hand, V_1 starts to decrease after LHRF injection with a time lag of 200msec. From these data, the current profile is estimated using the diffusion equation of poloidal magnetic field [20]. The

calculation result is illustrated in Fig. 13(b), (c). Fig. 13(b) is the current profiles of each time calculated to fit the time dependencies of l_i, V_1 shown in Fig. (c). These figures indicate that at first the effect of LHCD begins to appear at edge of the plasma because the time constant L/R at the edge is lower than that at the center due to $R_{edge} > R_{center}$ as $R \sim T_e^{-3/2}$. Therefore, the current in the edge region disappear at first and the l_i increases. Successively, the current component except the LHCD current at the center region decreases gradually and the current profile becomes broad. The experimental transition of Λ is explained well by the simple diffusion model of poloidal magnetic field, though a more physical and quantitative model is necessary. Fig. 14 is the measured dependences of $\Delta\Lambda_{LH}$ on $P_{LH}/(T_e n_e)$. Here, $\Delta\Lambda_{LH}$ is defined as $\Delta\Lambda_{LH} \equiv \Lambda_{\text{after LHCD}} - \Lambda_{\text{before LHCD}}$, which indicates the change of current profile. When $\Delta\Lambda < 0$, the profile becomes broad, conversly when $\Delta\Lambda > 0$, the profile becomes sharp. This figure indicates that if P_{LH} is relatively high, the current profile is flat and if P_{LH} is low, the profile is sharp, which strongly suggests the possibility of current profile control by LHCD power. Furthermore, as well as P_{LH}, the other parameters like $N_{//}$, frequency, B_t can be used for current profile control. In addition to the profile control, the suppression of MHD modes was observed on JT-60 as well as ASDEX, PETULA and PLT [13-15]. Fig. 15(a) is the time dependent signal of soft X-rays along with V_1, Λ, $\bar{n}_e$ and P_{RF}. It is clearly shown that the sawtooth on the soft X-ray signal is suppressed by LHRF injection of P_{RF}=450kW at t≧3.06sec. Also, the signal of $d\tilde{B}_\theta/dt$, which is a vibration of poloidal magnetic field $\sim\omega\tilde{B}_\theta$ is given in Fig. 15(b). In this experiment, LHRF of $P_{RF} = 1.0$MW was first injected into the plasma of $I_p = 1.0$MA, and NB of $P_{NBI} = 4.9$MW is injected from t = 5.1sec, subsequently. As soon as LHCD is turned off (while NBI is still injecting), $\tilde{B}_\theta$ grows to a large value. Though we cannot distinguish the mode number of $\tilde{B}_\theta$, probably the change of $\tilde{B}_\theta$ depends not on the amplitude of $\tilde{B}_\theta$ but on the change of frequency of rotation of plasma in poloidal direction. So, the figure indicates that LHCD effectively suppresses the enhancement of frequency of plasma rotation by NBI. These results may give us the possibility of improvement of plasma confinement by LHCD [20,21].

6. Summary

The LHCD current drive experiment on JT-60 provides the first results on a reactor grade tokamak and has confirmed the potential of current drive by LHRF seen in small and middle sized tokamaks. The main results obtained in this experiment are as follows;

(1) The plasma current of I_{RF}=1.7MA was driven by LHRF with the power of $P_{LH} = 1.2$MW at $I_p = 2$MA, $\bar{n}_e \sim 0.3 \times 10^{19}$ m^{-3}.

(2) Recharging and current ramp up was demonstrated. The ramp up efficiency and the recharging efficiency are estimated to be $\eta_{RAMP} = 0.2$ and $\eta_{recharge} = 0.2$.

(3) The current drive efficiency η_{CD} is $\eta_{CD} = 1.0 \sim 1.7$. This value is higher than the data of other small or middle sized tokamak $\eta_{CD} = 0.5 \sim 1.5$. This may be due to the effect of high electron temperature.

(4) The current drive efficiency was improved by the combination of LHCD with NBI. Then η_{CD} increased from 1.0 ~ 1.7 to 2.0 ~ 2.8.

(5) The current profile broadened for relatively high P_{LH}. ($P_{LH} > 2n_{19}I_p$)

(6) The suppression of sawtooth on the soft X-ray signal and $\tilde{B}_\theta$ by LHCD was obserbed.

Acknowledgement

The authers wish to thank the members of JAERI who have contributed to the JT-60 project. We also would like to thank Dr. S. Mori, Dr. Y. Iso, Dr. K. Tomabechi, Dr. M. Yoshikawa and Dr. T. Iijima.

6. Summary

The LHCD current drive experiment on JT-60 provides the first results on a reactor grade tokamak and has confirmed the potential of current drive by LHRF seen in small and middle sized tokamaks. The main results obtained in this experiment are as follows;

(1) The plasma current of I_{RF}=1.7MA was driven by LHRF with the power of $P_{LH} = 1.2$MW at $I_p = 2$MA, $\bar{n}_e \sim 0.3 \times 10^{19}$ m^{-3}.

(2) Recharging and current ramp up was demonstrated. The ramp up efficiency and the recharging efficiency are estimated to be $\eta_{RAMP} = 0.2$ and $\eta_{recharge} = 0.2$.

(3) The current drive efficiency η_{CD} is $\eta_{CD} = 1.0 \sim 1.7$. This value is higher than the data of other small or middle sized tokamak $\eta_{CD} = 0.5 \sim 1.5$. This may be due to the effect of high electron temperature.

(4) The current drive efficiency was improved by the combination of LHCD with NBI. Then η_{CD} increased from 1.0 ~ 1.7 to 2.0 ~ 2.8.

(5) The current profile broadened for relatively high P_{LH}. ($P_{LH} > 2n_{19}I_p$)

(6) The suppression of sawtooth on the soft X-ray signal and $\tilde{B}_\theta$ by LHCD was obserbed.

Acknowledgement

The authers wish to thank the members of JAERI who have contributed to the JT-60 project. We also would like to thank Dr. S. Mori, Dr. Y. Iso, Dr. K. Tomabechi, Dr. M. Yoshikawa and Dr. T. Iijima.

References

[1] T. Yamamoto, T. Imai, et al., Phys. Rev. Lett., 45 (1980) 716.
[2] T. Maekawa et al. Phys. Rev. Lett. 85A (1981) 339.
[3] K. Okubo, et al., Nucl. Fusion 22 (1982) 203.
[4] S. Beranabei, et al., Phys. Rev. Lett. 49 (1982) 1255.
[5] M. Porkolab, et al., in Proc. of 9th Inter. Conf. on plasma Physics and Controlled Nuclear Fusion Research, Baltimore, 1982 (IAEA, Vienna, 1983) Vol. 1, p.227.
[6] S. Luckhardt., et al., Phys. Rev. Lett. 48 (1982) 152.
[7] G. Tonon, et al., Proc. of the 9th Int. Conf. on Plasma Physics and Controlled Fusion, Baltimore, 1982 (IAEA, Vienna, 1983) Vol. 1, p.439.
[8] F. Jobes, et al., Phys. Rev. Lett., 52 (1984) 1005.
[9] T.K. Chu, et al., Proc. of 4th Int. Symp. on Heating in Toroidal Plasma, Roma (1984) Vol. 1, p.529.
[10] M. Porkolab et al., ibid 4. vol. 1, p.529.
[11] F. Leuterer, et al., Proc. of 10th Conf. on Plasma Physics and Controlled Nuclear Fusion Research, London, 1984 (IAEA, Vienna, 1985) Vol. 1, p.597.
[12] B. Coppi, Comments on Plasma Phys. Control Fusion, 1980, Vol. 5, p.261-p.270.
[13] D. Van Houtte, et al., Nuclear Fusion 24 (1984) 1485.
[14] T.K. Chu, et al., Sixth Topical Conf. on Radio Freq. Plasma Heating, May 13-15 1985, Pine Mountain (USA).
[15] F.X. Söldner, et al., in Proc. of 12th European Conference on Controlled Fusion and Plasma Physics, Budapest, 1985, Vol. 2, p.172.
[16] N.J. Fisch, Phys. Rev. Lett. 41 (1978) 873.
[17] N.J. Fisch, Phys. of Fluids 28 (1) January (1985) 245.
[18] G. Tonon, 11th European Conf., Aachen, Sept 83, Plasma Physics and Controlled Fusion, Jan. 1984, Vol. 26, p.145.
[19] M. Porkolab, IEEE Trans, on Plasma Science, Vol. PS-12, No.2, June (1984) 107.
[20] K. Ushigusa, et al., JAERI-M report 87-012.
[21] T. Imai, et al., Proc. of 11th Int. Conf. on Plasma Physics and Controlled Fusion Research, Kyoto 1986, in Press.

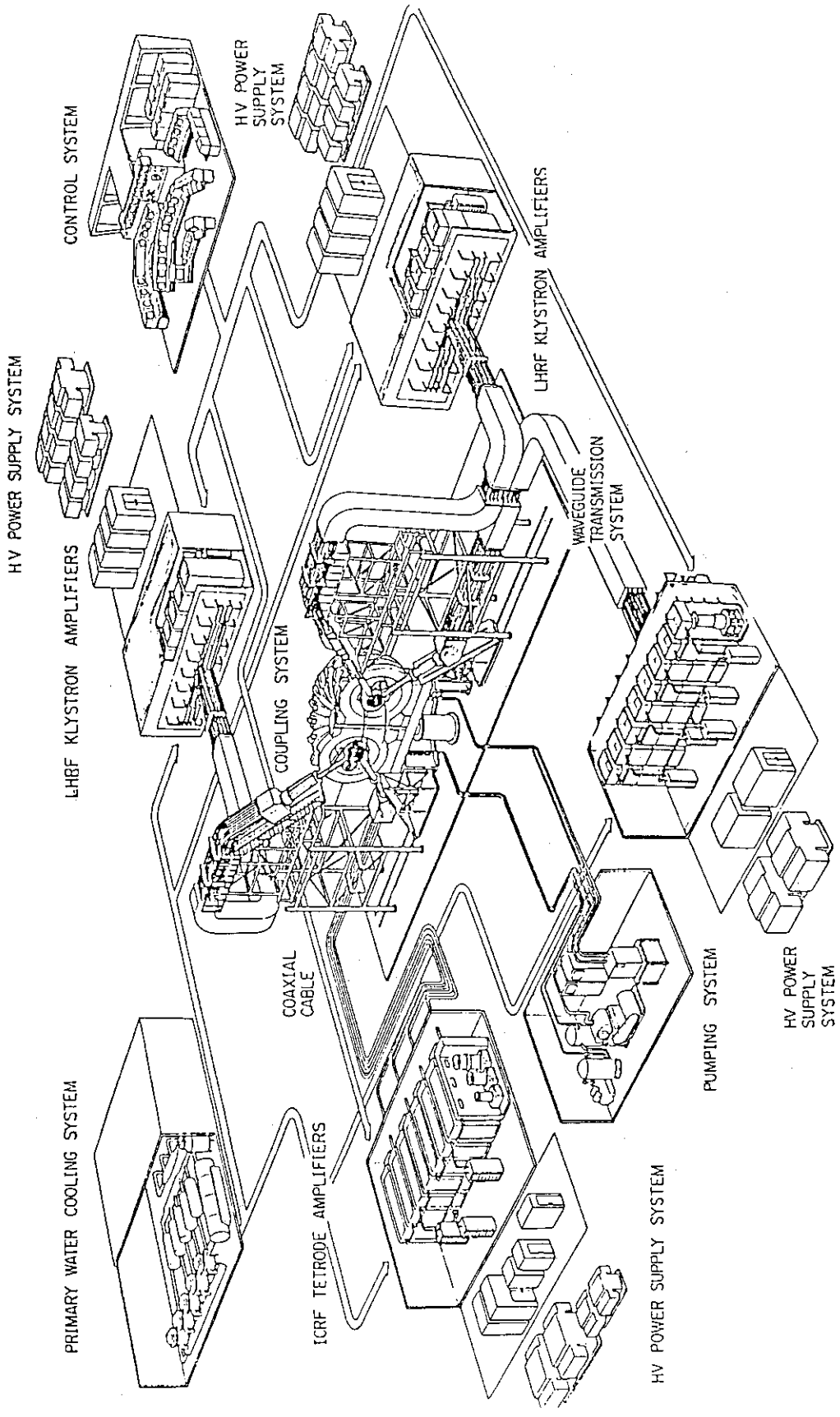

Fig.1 The layout of RF heating system.

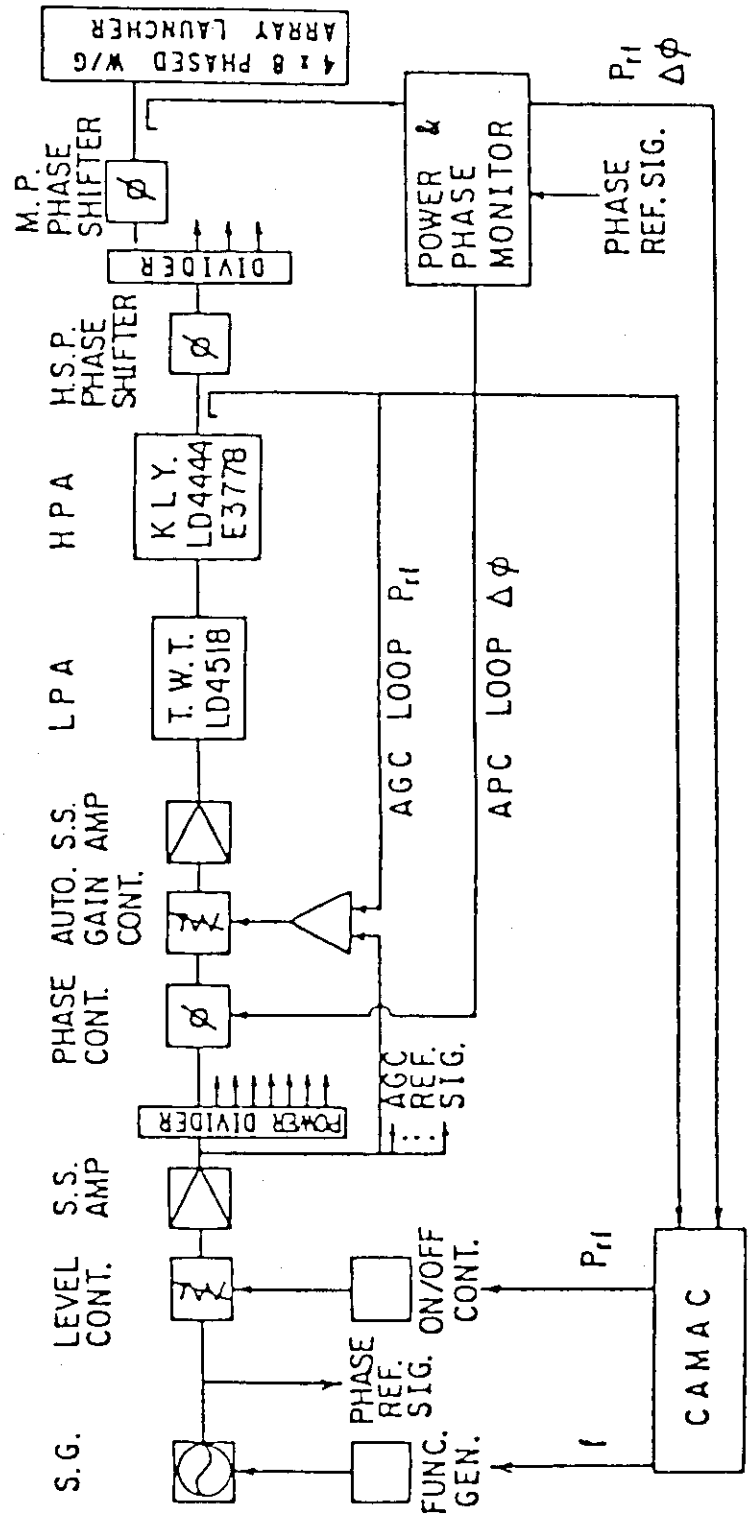

Fig.2 The line-up of high power RF generating system.

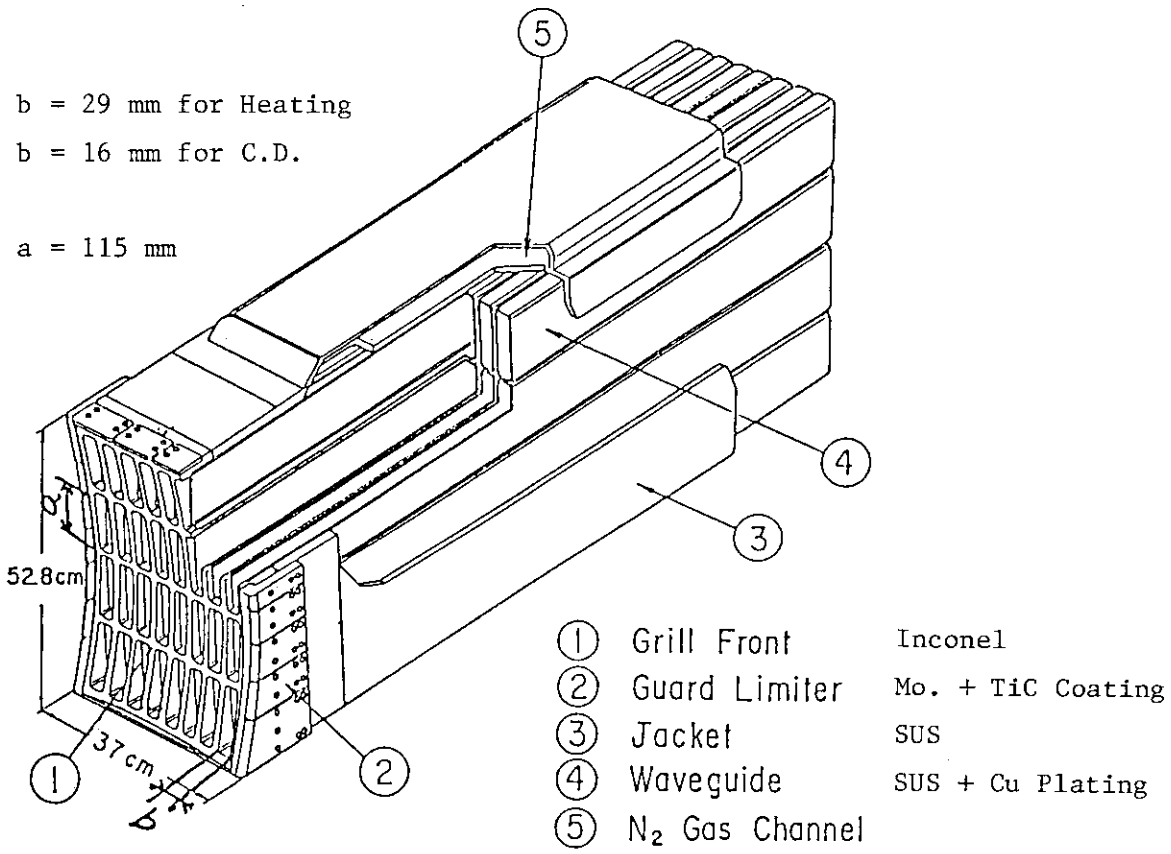

(a)

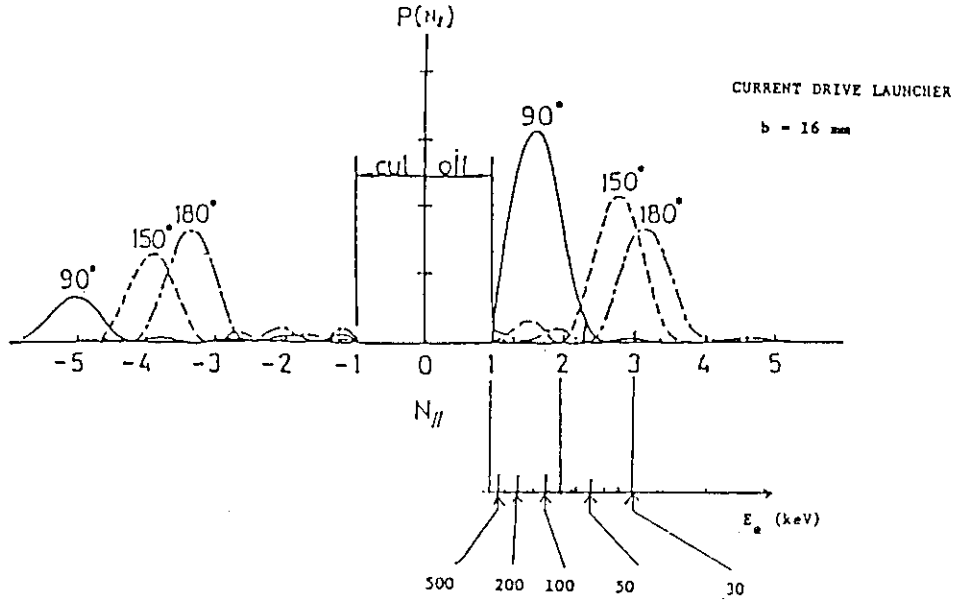

(b)

Fig.3 (a) The picture of the top of the launcher.
(b) The power spectrum as the refraction along the magnetic field $N_{//}$.

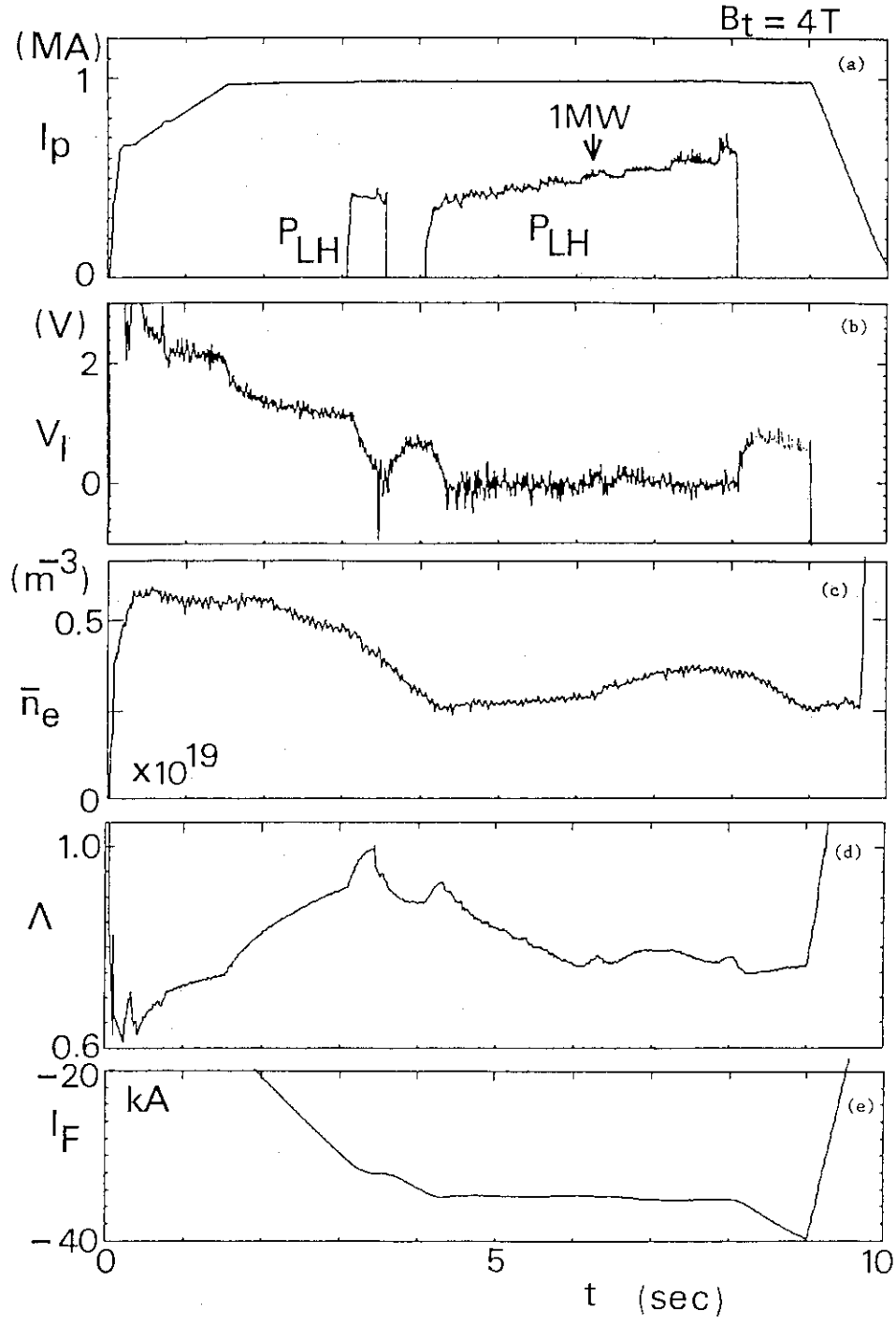

Fig. 4 Typical time dependences of plasma parameters in the current drive experiment under I_p constant control at P_{LH}=1MW, B_T=4T with hydrogen plasma.

(a) plasma current I_p and RF power

(b) one turn voltage V_1

(c) electron density $\bar{n}_e$

(d) Shafranov lambda Λ

(f) current of OH I_F

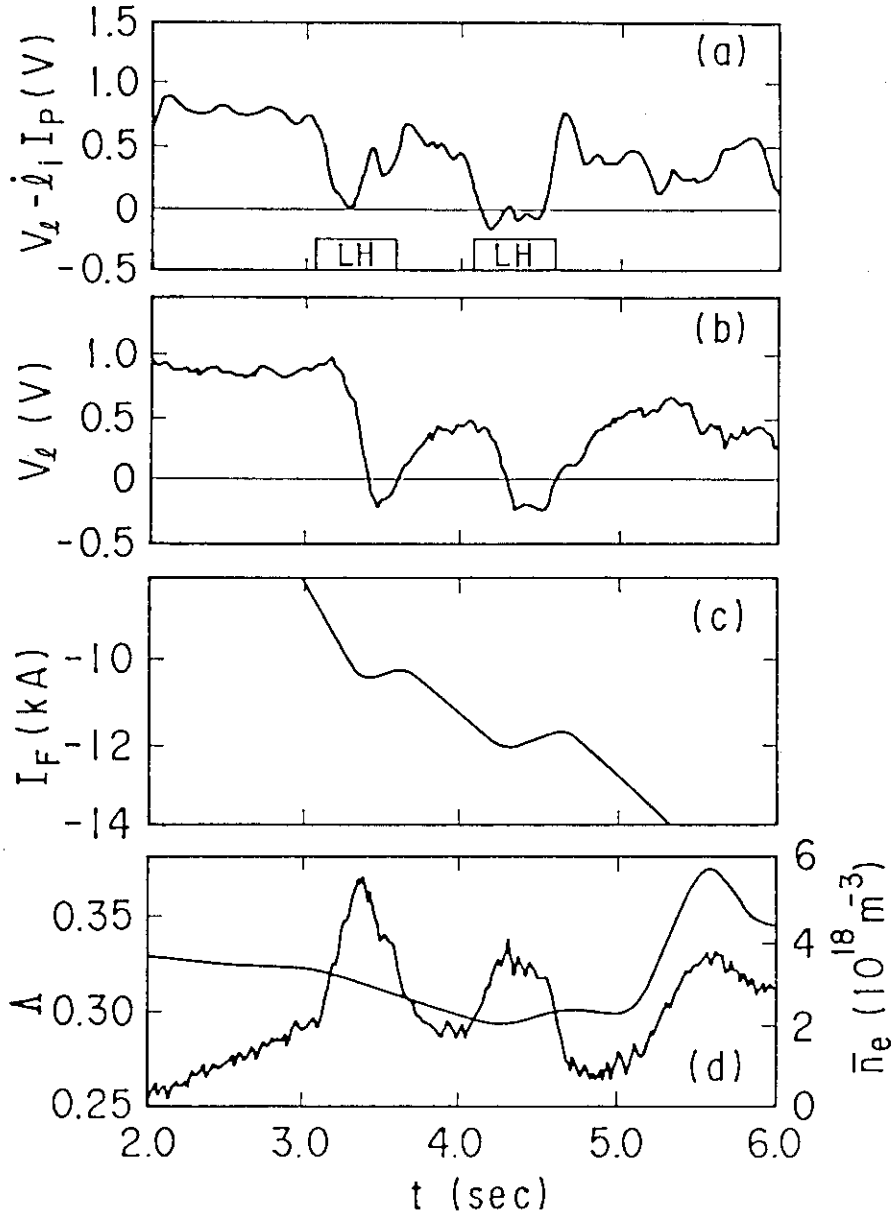

Fig.5 Time dependences of V_l and I_F in recharging by LHCD.
(a) $V_l - \dot{l}_i I_p$ and LHRF power
(b) I_F and RF power
(c) OH coil current I_F
(d) Λ $(=\beta_p + l_i/2)$ and density

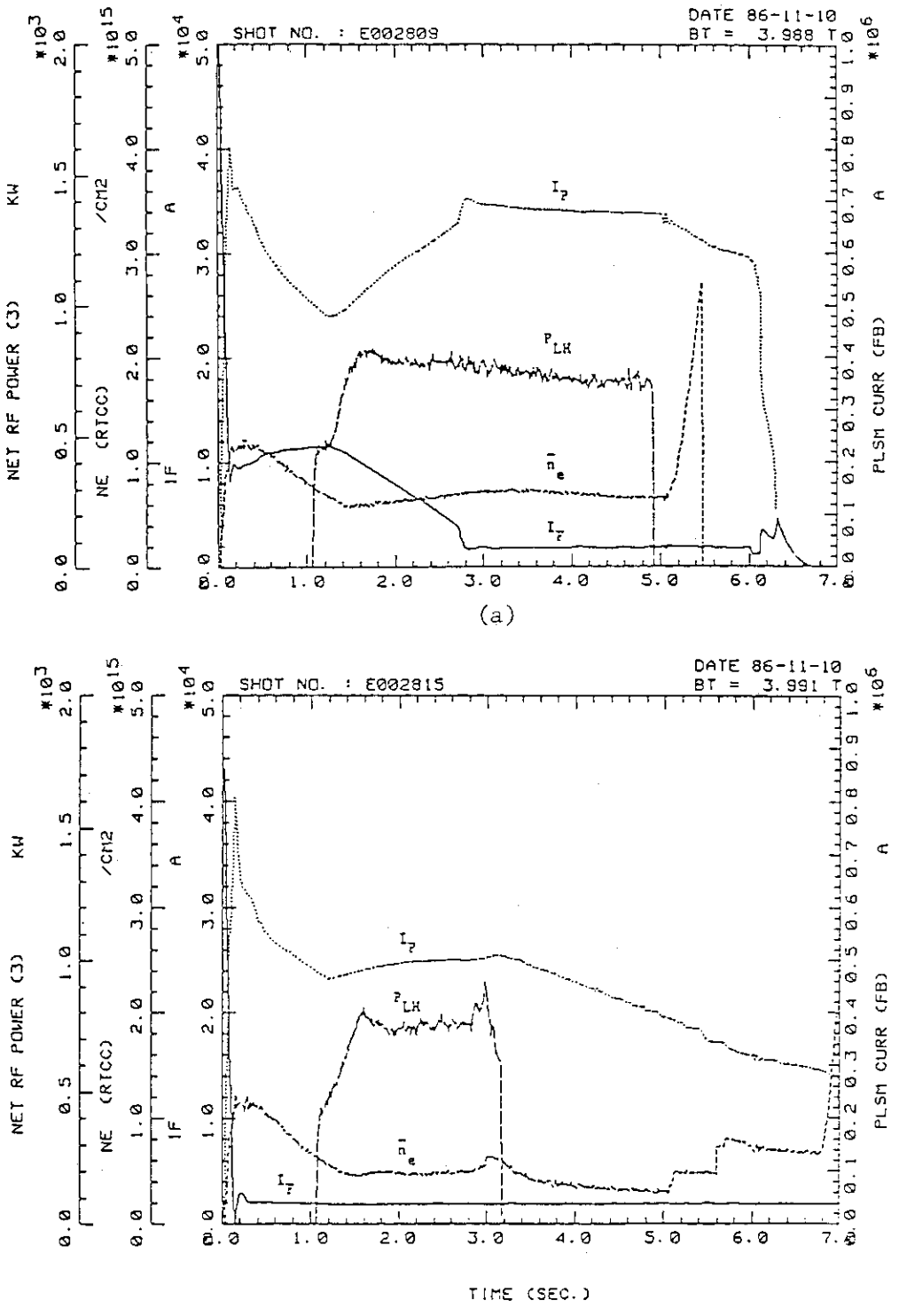

Fig.6 Time dependence of I_p, I_F line density in the case of current sustain and current ramp up by LHCD without I_p constant control.

(a) current sustain

(b) current ramp up

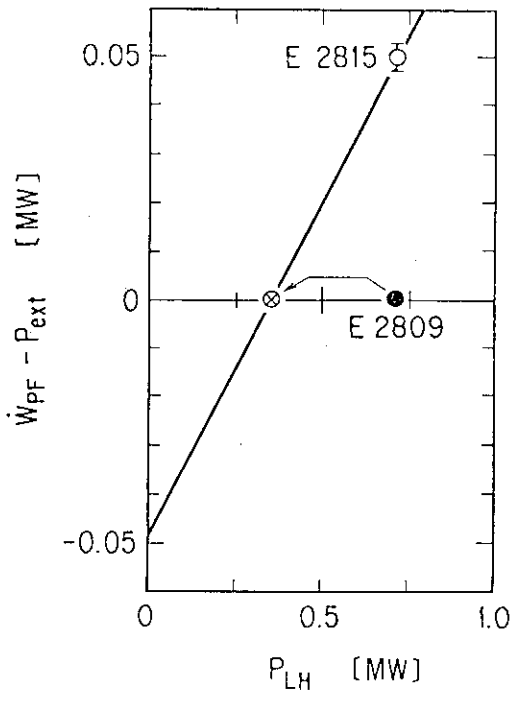

Fig.7 $dW_{PF}/dt-P_{ext}$ v.s. P_{RF} in the current ramp up experiment. The gradient of the solid line indicates the ramp up efficiency $\eta_{ramp} = 0.2$. The data shown by ○ E2815 and ● E2809 are obtained with $I_p = 0.5$ MA, $\bar{n}_e = 0.28 \times 10^{19} m^{-3}$ and $I_p = 0.7$ MA, $\bar{n}_e = 0.22 \times 10^{19} m^{-3}$, respectively. The point shown by ⊗ is the value when as evaluated on the same condition with E2815.

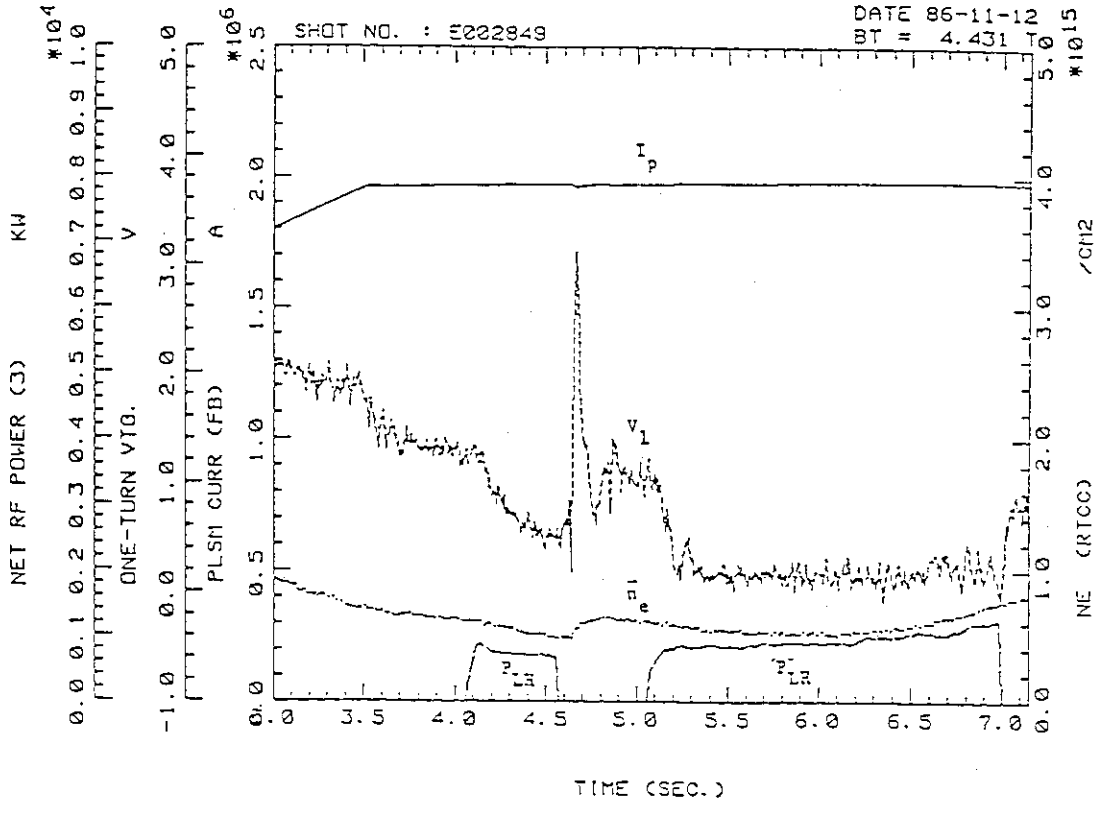

Fig.8 The data of 1.7 MA current drive. The time dependences of I_p, V_1 and line density are shown.

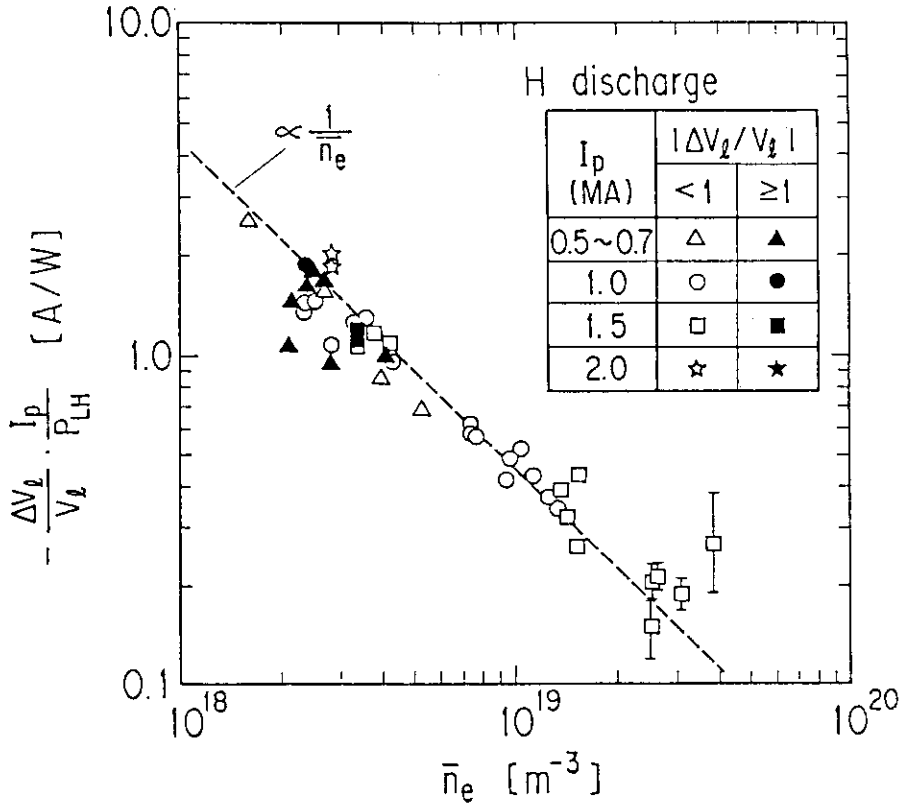

(a)

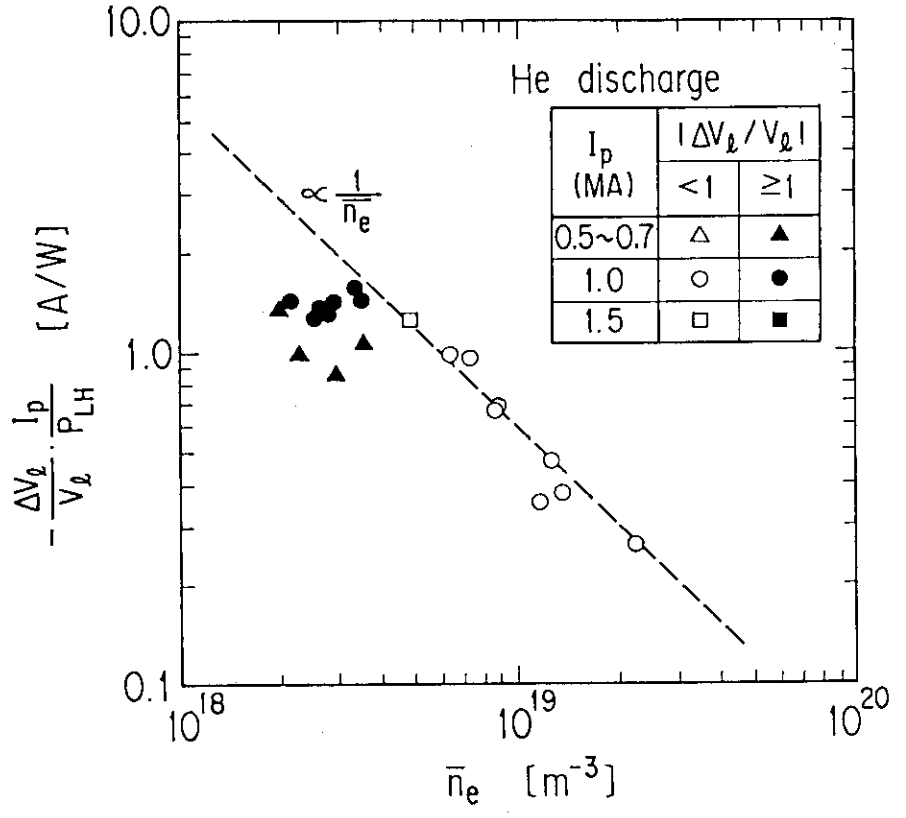

(b)

Fig. 9 $I_p \Delta V_\ell / (V_\ell P_{LH})$ vs. $\bar{n}_e$
(a) H discharge
(b) He discharge

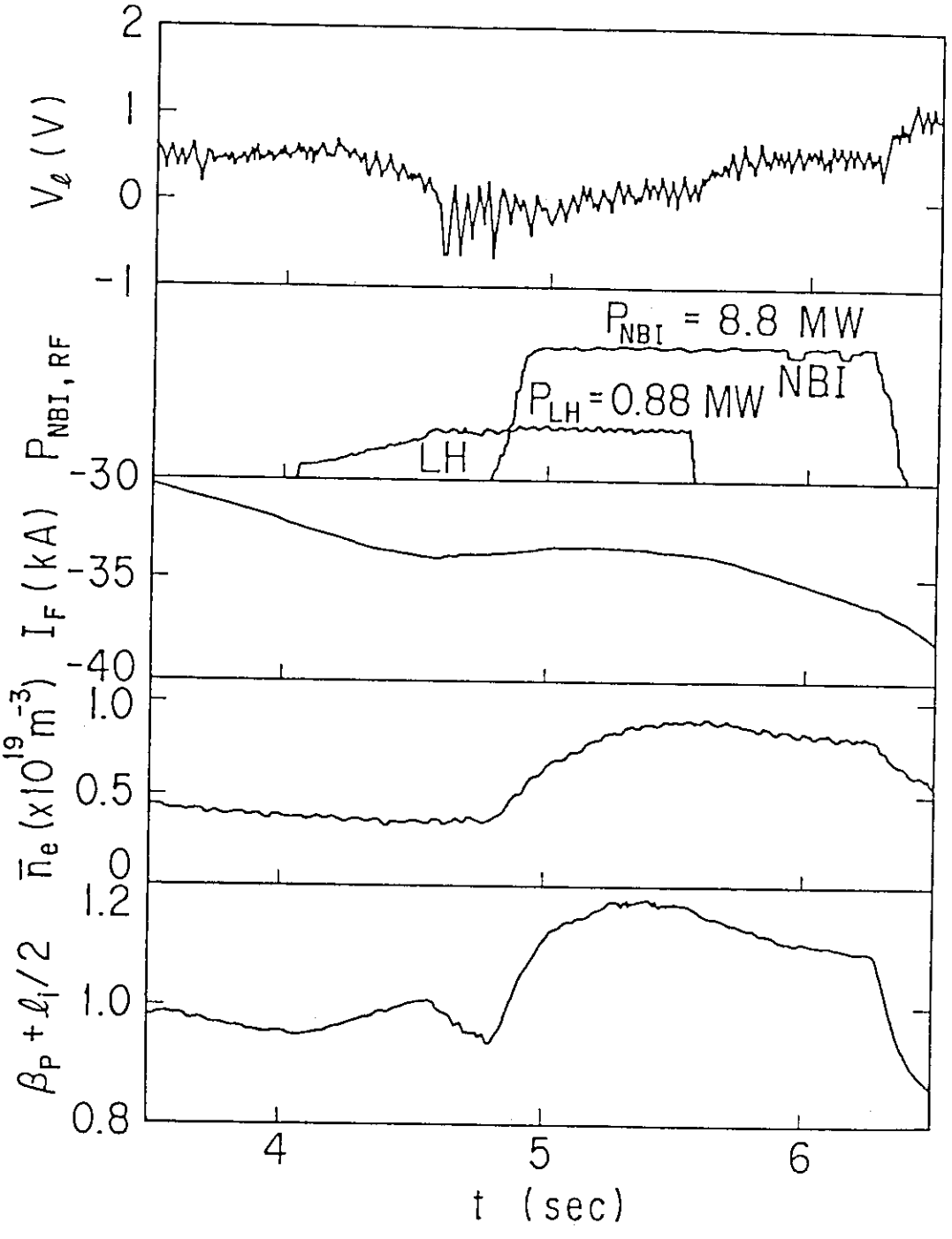

Fig.10 Typical data of time dependence of plasma parameters in OH+LHCD+NBI shot. From top figure, V_l, powers of NBI and RF, $\bar{n}_e$ and $\beta_p+l_i/2$ are shown.

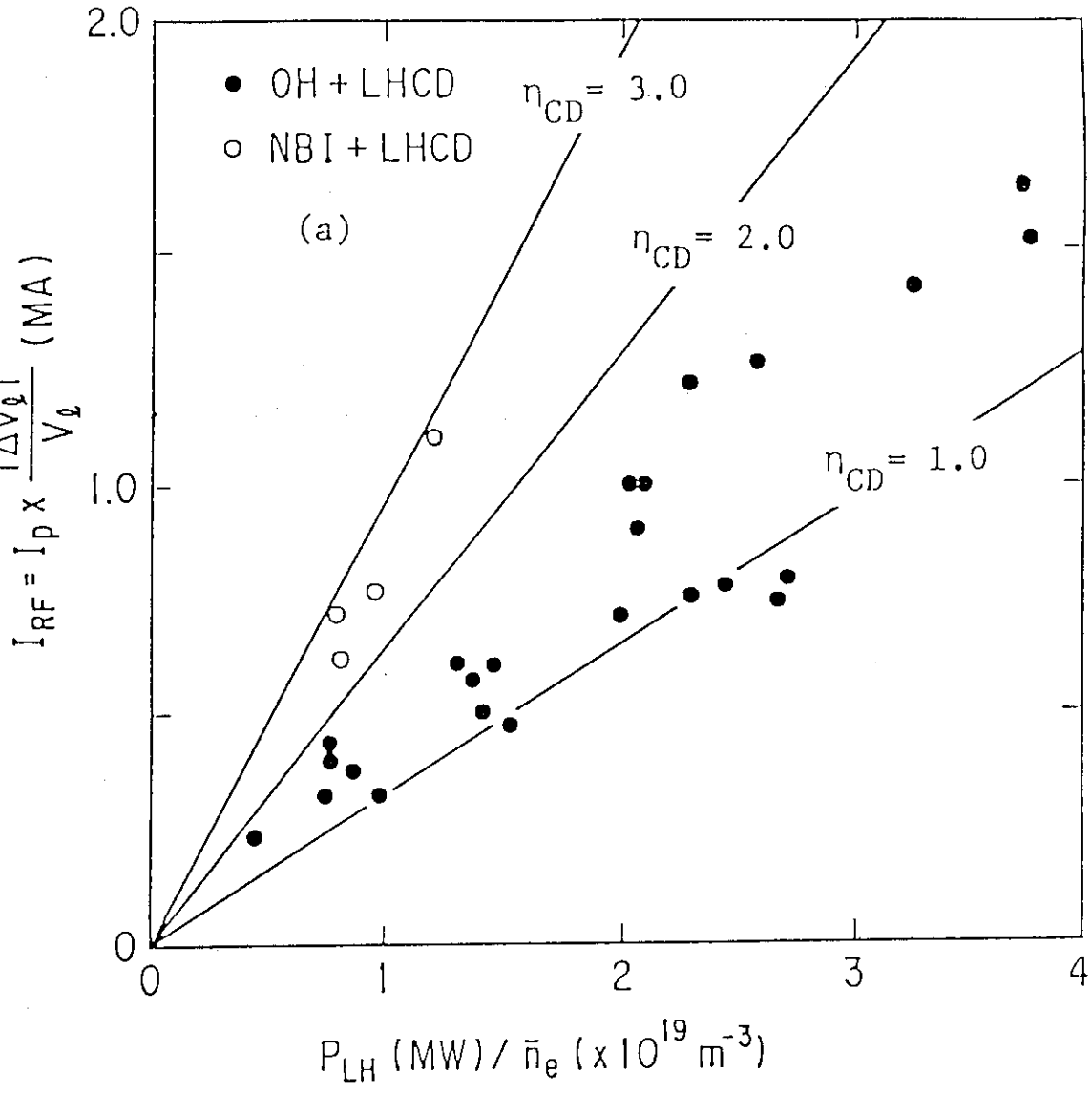

Fig.11 I_{RF} vs. $P_{LH}/\bar{n}_e$ for OH+LHCD only(●) and OH+LHCD+NBI(○). The solid lines indicates η_{CD}=1.0,2.0,3.0 as shown in the figure.

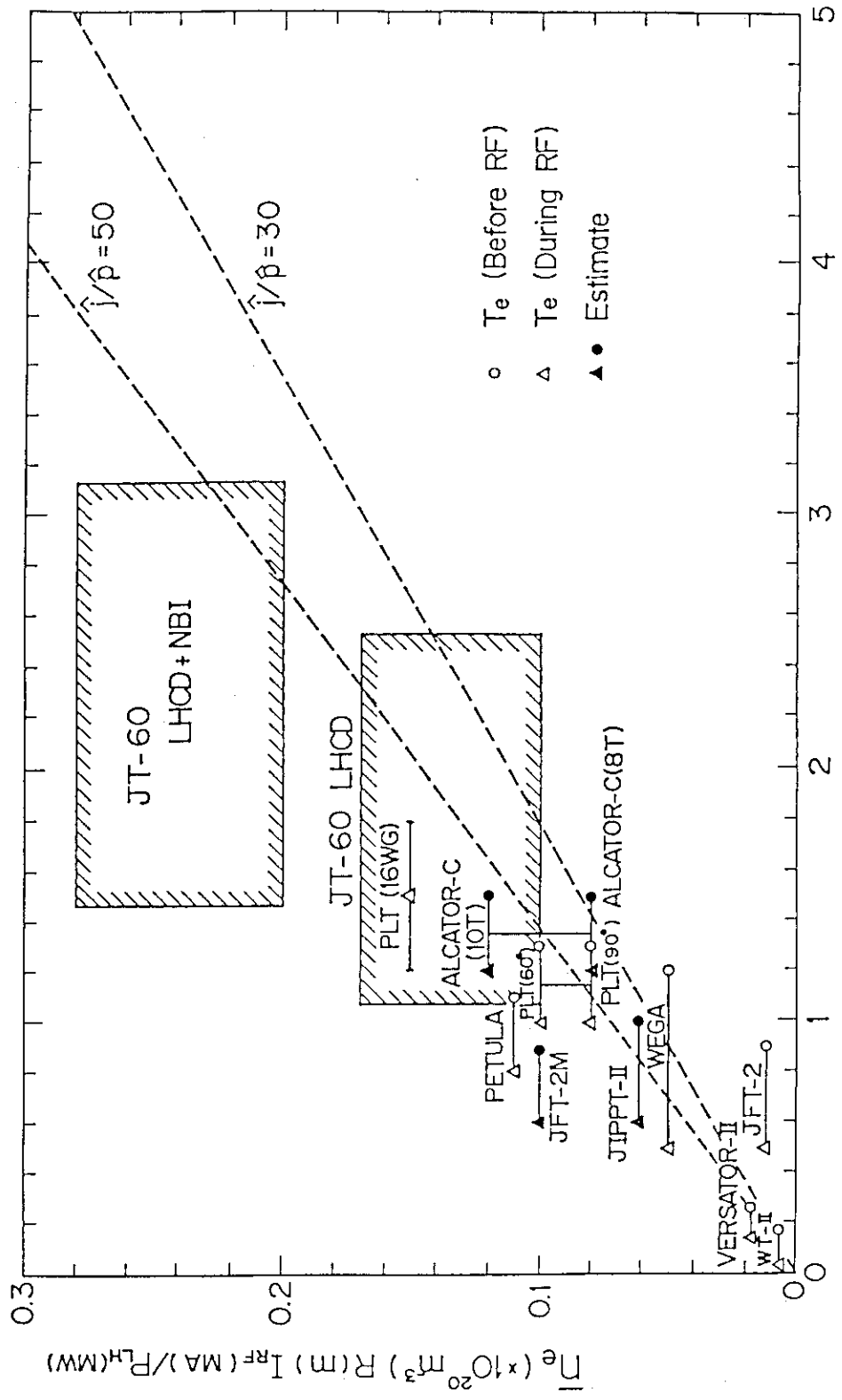

Fig.12 The temperature dependence of current drive efficiency (= $\bar{n}_e R I_{RF}/P_{LH}$). The simbols of ○, △ mean the temperature before and after RF injection, respectively. The closed symbols are estimated values. The dashed lines shows the characteristic current drive efficiency.

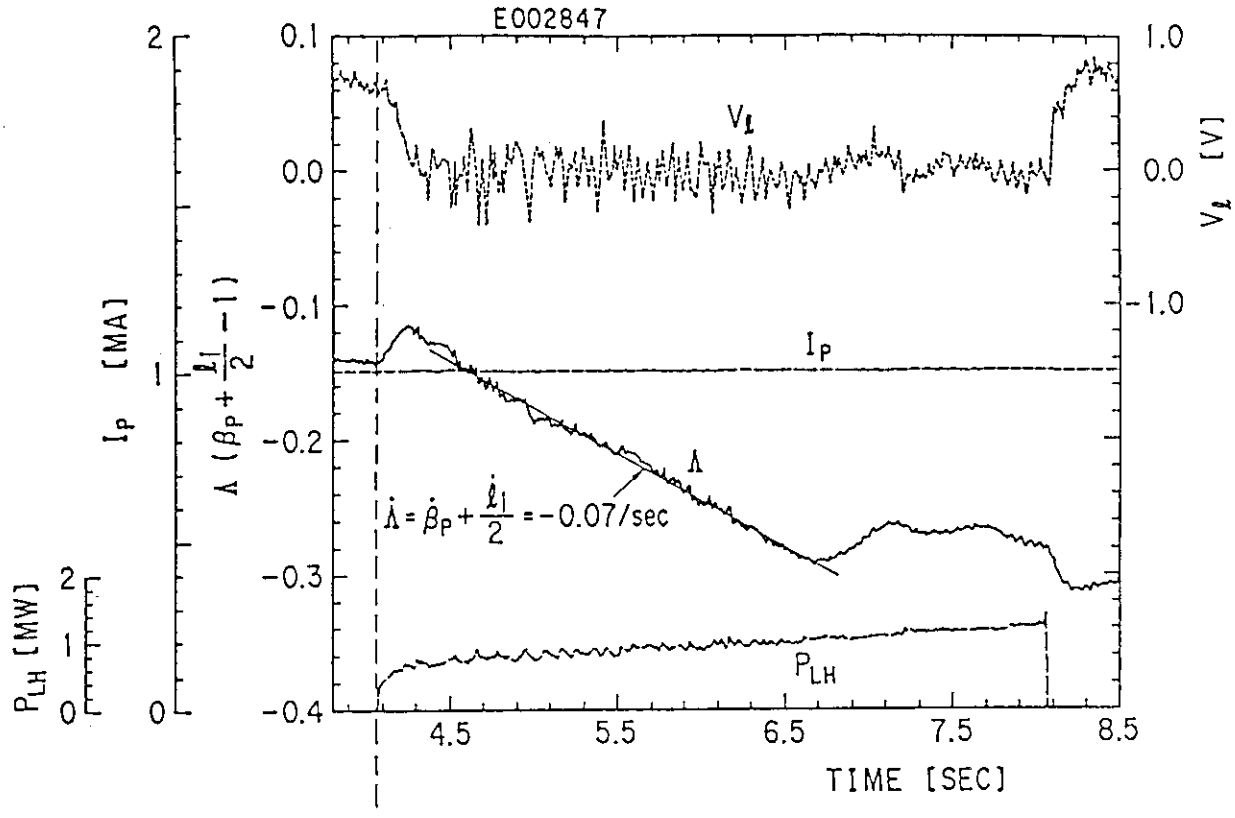

Fig.13 (a) Typical experimental results of time dependences of V_1, Λ.

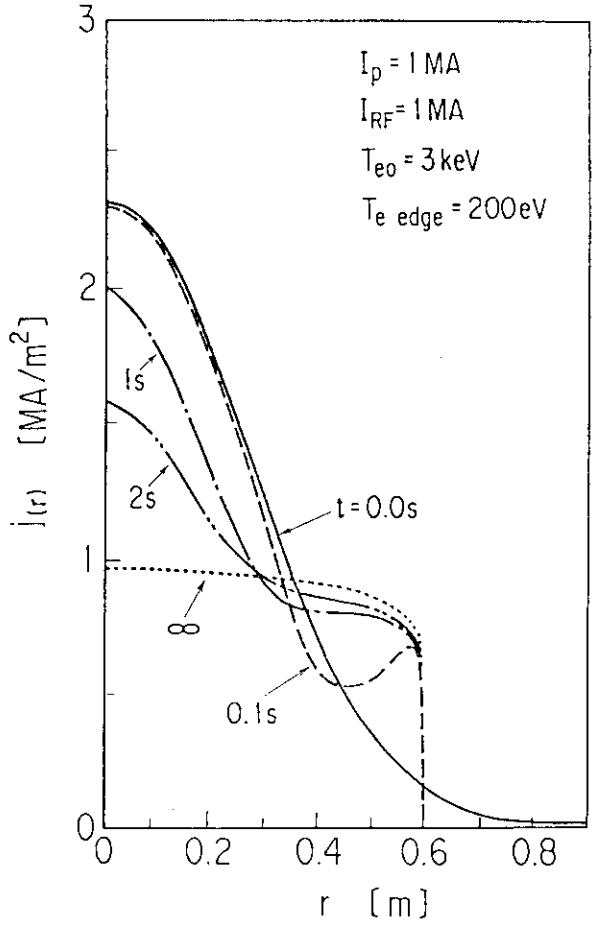

(b)

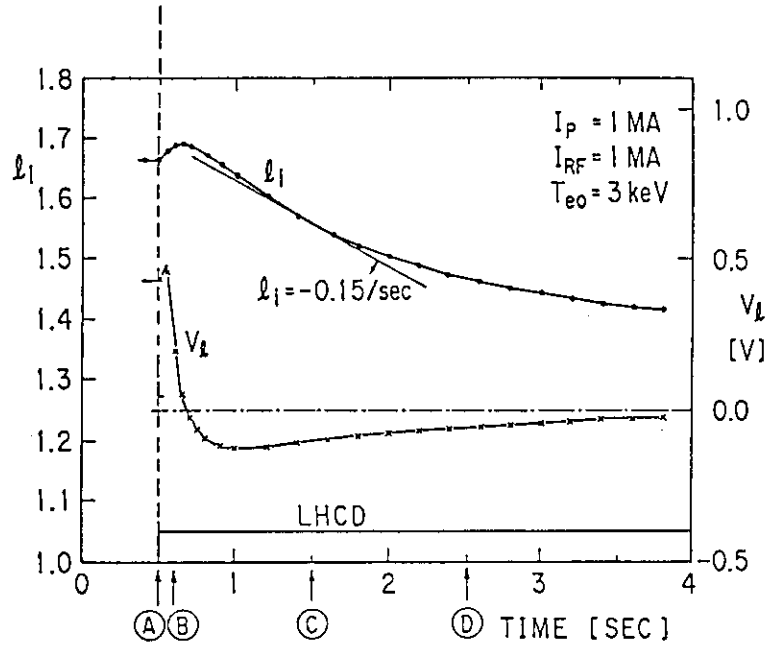

(c)

Fig.13 (b) The current profiles at each time calculated using the diffusion equation of poloidal magnetic field to fit to the time dependences of l_i and V_i shows in (c).

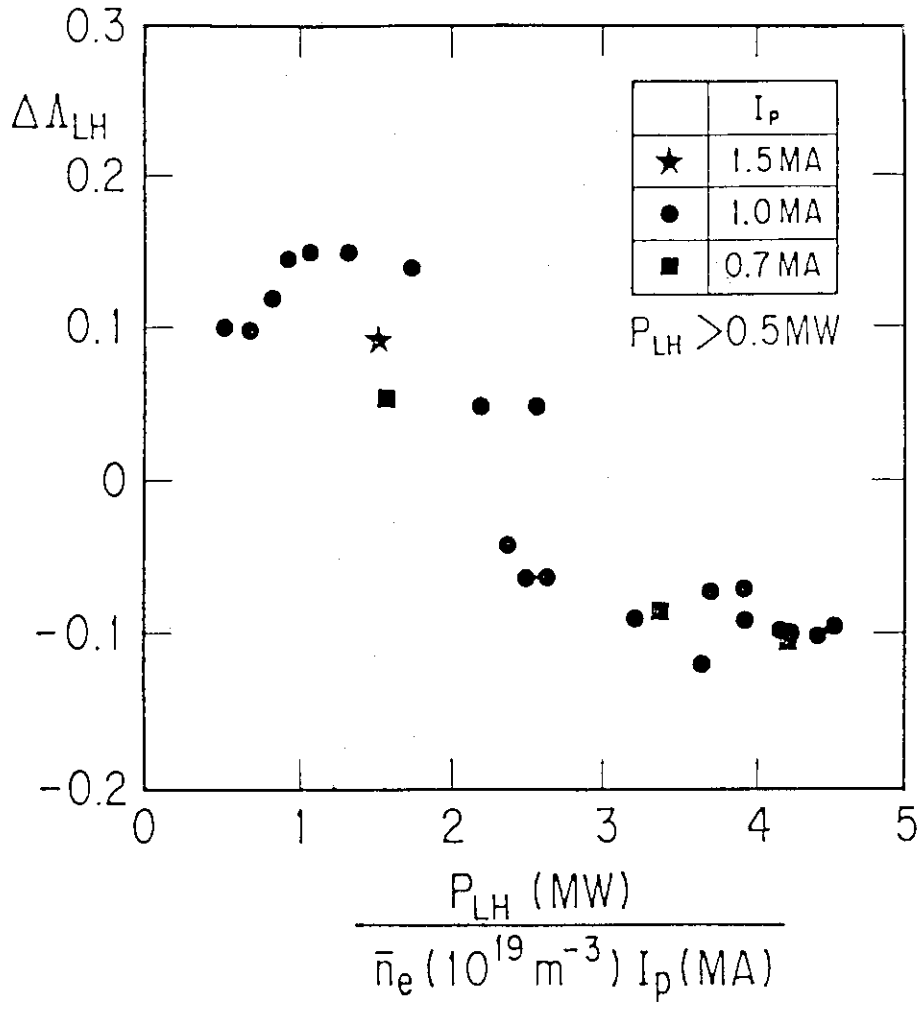

Fig.14 Dependence of $\Delta\Lambda_{LH}$ ($=\Lambda_{\text{after LHCH}}-\Lambda_{\text{before LHCD}}$) on P_{LH}/n_eI_p.

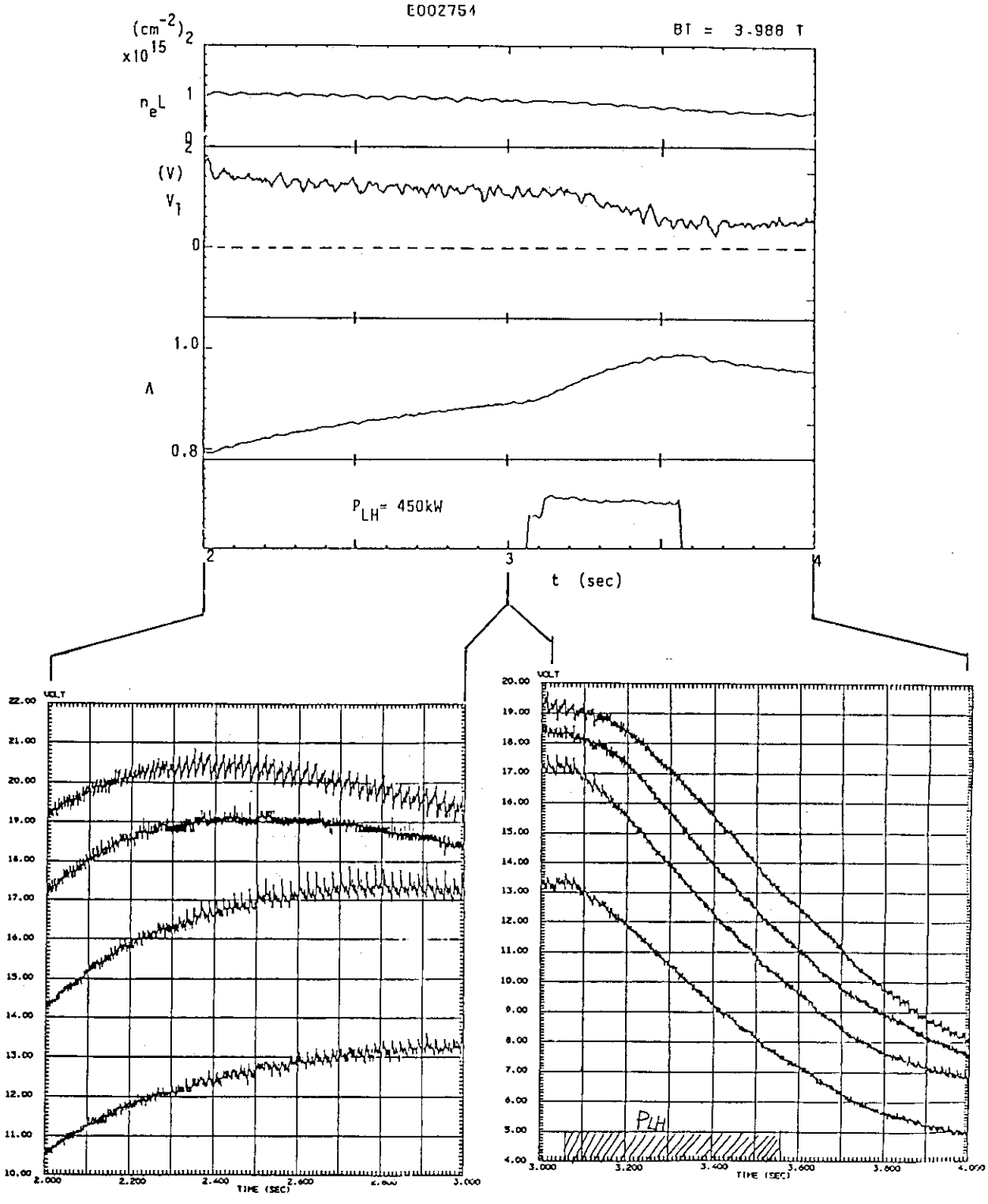

Fig.15 Time dependences of soft X-ray and $d\tilde{B}_\theta/dt$.
(a) soft X-ray with V_1, Λ, $\bar{n}_e$ and P_{RF}. The power of RF is 450 kW.

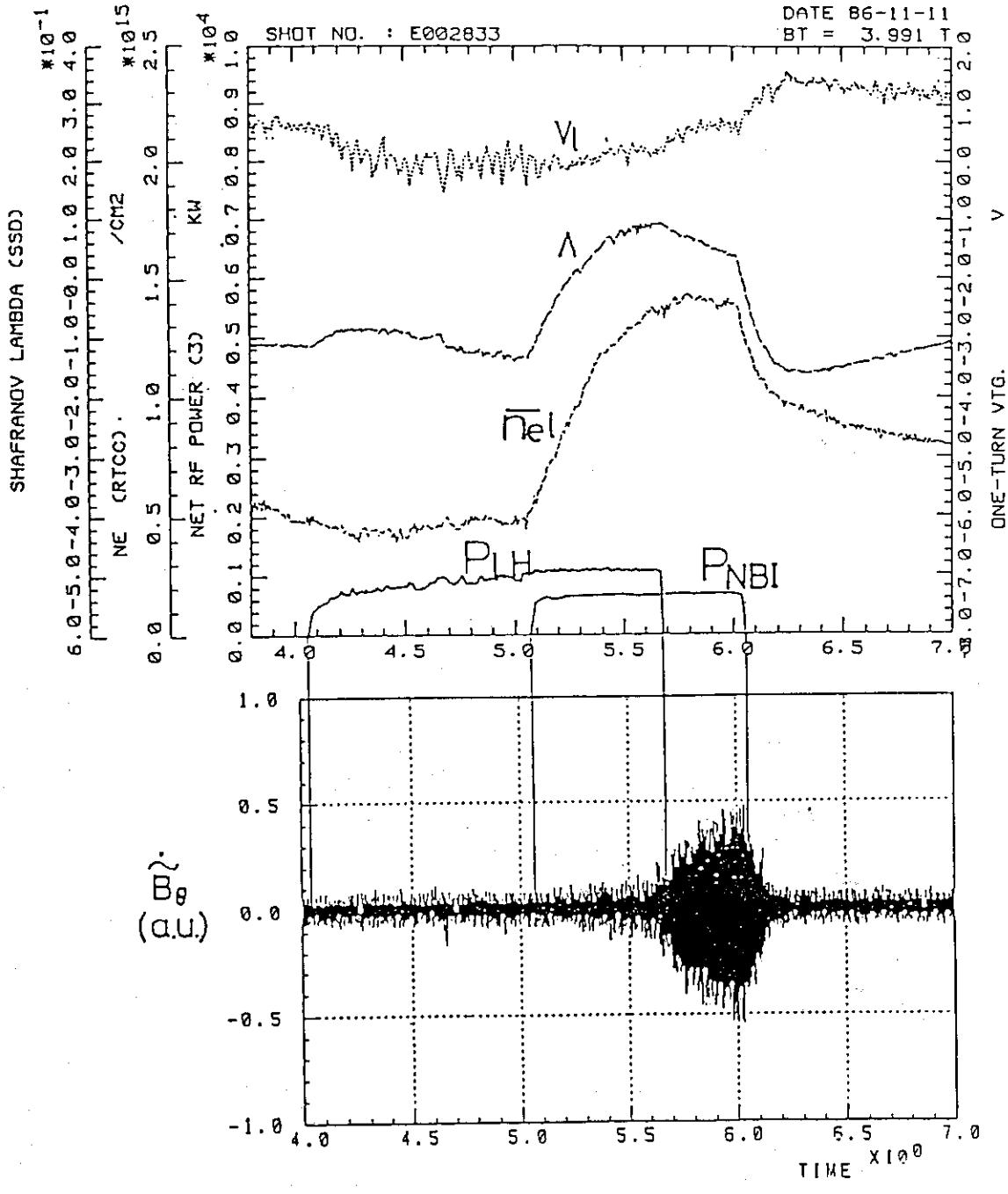

Fig.15 Time dependences of soft X-ray and $d\tilde{B}_\theta/dt$.
(b) $d\tilde{B}_\theta/dt$ and with the time transition of V_1, $\bar{n}_e$, Λ and powers of RF and NBI. Here, $P_{RF} = 1.0$ MW and $P_{NBI} = 4.9$ MW.